Molecular Pharmacology Fast Forward. Published on October 13, 2015 as DOI: 10.1124/mol.115.100529
This article has not been copyedited and formatted. The final version may differ from this version.

Title Page

A small molecule pyrazolo[3,4-*d*]pyrimidinone inhibitor of zipper-interacting protein kinase suppresses calcium sensitization of vascular smooth muscle

Justin A. MacDonald, Cindy Sutherland, David A. Carlson, Sabreena Bhaidani, Abdulhameed Al-Ghabkari, Karl Swärd, Timothy A. J. Haystead, and Michael P. Walsh

Department of Biochemistry & Molecular Biology, University of Calgary, Cumming School of Medicine, 3280 Hospital Drive NW, Calgary, AB, T2N 4Z6, Canada (JAM, CS, SB, AA-G, MPW), Department of Experimental Medical Science, BMC D12, Lund University, Lund, Sweden (KS), and Department of Pharmacology & Cancer Biology, Duke University Medical Center, Durham, NC 27710, USA (DAC, TAJH)

Molecular Pharmacology Fast Forward. Published on October 13, 2015 as DOI: 10.1124/mol.115.100529
This article has not been copyedited and formatted. The final version may differ from this version.

Running Title Page

Running Title: ZIPK and vascular smooth muscle contraction

To whom correspondence should be addressed: Justin A. MacDonald, Smooth Muscle Research Group at the Libin Cardiovascular Institute of Alberta, University of Calgary, Cumming School of Medicine, 3280 Hospital Drive NW, Calgary, AB, T2N 4Z6; Tel: 403-210-8433, E-mail: jmacdo@ucalgary.ca

# of text pages: 38

# of figures: 10

Abstract word count: 239

Introduction word count: 752

Discussion word count: 1523

Abbreviations: AngII, angiotensin II; CLa, calyculin A; CPI-17, protein kinase C-potentiated inhibitory protein for myosin phosphatase of 17 kDa; DAPK, death-associated protein kinase; DTT, dithiothreitol; ET-1, endothelin-1; ILK, integrin-linked kinase; LC_{20}, myosin 20-kDa regulatory light chain; LZ, leucine zipper motif; MLCK, myosin light chain kinase; MLCP, myosin light chain phosphatase; MYPT1, myosin phosphatase-targeting subunit 1; Par-4, prostate apoptosis response-4; PBS, phosphate-buffered saline; PIM kinases, proviral integrations of Moloney virus kinases; PKC, protein kinase C; PVDF, polyvinylidene difluoride; ROCK, Rho-associated coiled coil-containing protein kinase; TCA, trichloroacetic acid; VSM, vascular smooth muscle; ZIPK, zipper-interacting protein kinase

Molecular Pharmacology Fast Forward. Published on October 13, 2015 as DOI: 10.1124/mol.115.100529
This article has not been copyedited and formatted. The final version may differ from this version.

Abstract

A novel inhibitor of zipper-interacting protein kinase (ZIPK) was utilized to examine the involvement of ZIPK in the regulation of smooth muscle contraction. Pre-treatment of de-endothelialized rat caudal arterial smooth muscle strips with the pyrazolo[3,4-*d*]pyrimidinone inhibitor HS38 decreased the velocity of contraction (time to reach half-maximal force) induced by the phosphatase inhibitor calyculin A in the presence of Ca^{2+} without affecting maximal force development. This effect was reversed following washout of HS38 and correlated with a reduction in the rate of phosphorylation of LC_{20} (myosin 20-kDa regulatory light chains) but not of CPI-17 (protein kinase C-potentiated inhibitory protein for myosin phosphatase of 17 kDa), Par-4 (prostate apoptosis response-4) or MYPT1 (myosin phosphatase-targeting subunit 1), all of which have been implicated in the regulation of vascular contractility. A structural analog of HS38, with inhibitory activity towards PIM3 kinase but not ZIPK, had no effect on calyculin A-induced contraction or protein phosphorylations. We conclude that a pool of constitutively-active ZIPK is involved in regulation of vascular smooth muscle contraction through direct phosphorylation of LC_{20} upon inhibition of myosin light chain phosphatase activity. HS38 also significantly attenuated both phasic and tonic contractile responses elicited by phenylephrine, angiotensin II, endothelin-1, U46619 and K^+-induced membrane depolarization in the presence of Ca^{2+}, which correlated with inhibition of phosphorylation of LC_{20}, MYPT1 and CPI-17. These effects of HS38 suggest that ZIPK also lies downstream of G protein-coupled receptors that signal through both $G\alpha_{12/13}$ and $G\alpha_{q/11}$.

Molecular Pharmacology Fast Forward. Published on October 13, 2015 as DOI: 10.1124/mol.115.100529
This article has not been copyedited and formatted. The final version may differ from this version.

Introduction

The coordinated regulation of tone via protein kinases is a key functional property of vascular smooth muscle (VSM), and it is not surprising that a variety of signal transduction mechanisms can regulate VSM tone (Hirano, 2007; Kim et al., 2008; Wynne et al., 2009). Of central importance to VSM tone generation is the relationship between cytosolic Ca^{2+} concentrations ($[Ca^{2+}]_i$) and force generation. Greater force can be obtained in the absence of a change in $[Ca^{2+}]_i$ through a 'Ca^{2+} sensitization' process. Since blood flow is proportional to the fourth power of the vessel radius (Sutera and Skalak, 1993), fine control of VSM tone is essential for maintenance of normal cardiovascular function. This is achieved primarily via signaling pathways that lead to Ca^{2+} sensitization of the contractile response. Furthermore, alterations in the sensitivity of VSM cells to $[Ca^{2+}]_i$ have been hypothesized to underlie many cardiovascular diseases. For example, increased VSM contractility contributes to the severe arterial narrowing observed in vasospasm, chronic hypertension and the decreased dilatory responses of arteries in obesity, diabetes and aging (Georgescu et al., 2011; Katsumata et al., 1997; Masumoto et al., 2002; Takeya et al., 2014; Uehata et al., 1997).

The biochemical systems that govern Ca^{2+} sensitization in VSM are complex and multi-factorial, yet zipper-interacting protein kinase (ZIPK) has emerged as one of the most important. ZIPK has been linked to the regulation of diverse cellular processes, including cell motility, smooth muscle contraction and programmed cell death (reviewed in (Haystead, 2005; Ihara and MacDonald, 2007; Shiloh et al., 2014; Usui et al., 2014)). ZIPK possesses an *N*-terminal kinase domain, a central autoinhibitory region, a nuclear localization sequence and a *C*-terminal leucine zipper (LZ) motif. ZIPK (also known as

Molecular Pharmacology Fast Forward. Published on October 13, 2015 as DOI: 10.1124/mol.115.100529
This article has not been copyedited and formatted. The final version may differ from this version.

DAPK3) is a member of a larger family of protein kinases known as the death-associated protein kinases (DAPKs). The kinase domain is most closely related to other DAPK proteins but also shares significant sequence and structural conservation with calmodulin-dependent kinase family members such as myosin light chain kinase (MLCK) (Ihara et al., 2007; Moffat et al., 2011; Shiloh et al., 2014). In contrast to MLCK and the other DAPKs, ZIPK does not have a calmodulin-binding domain, and its activity is regulated independently of Ca^{2+}.

ZIPK appears to be a key regulator of VSM contractility, and the kinase is implicated in diphosphorylation of the 20-kDa regulatory light chain subunits of myosin II (LC_{20}) at Ser19 and Thr18 (Borman et al., 2002; Carlson et al., 2013; Moffat et al., 2011; Murata-Hori et al., 1999; Niiro and Ikebe, 2001), phosphorylation of the myosin phosphatase-targeting subunit (MYPT1) of myosin light chain phosphatase (MLCP) at the inhibitory sites, Thr697 and Thr855 (Endo et al., 2004; MacDonald et al., 2001a), and phosphorylation of the PKC-potentiated inhibitory protein for myosin phosphatase of 17 kDa (CPI-17) at Thr38 (MacDonald et al., 2001b). Ultimately, these targets are thought to be the primary mediators of ZIPK effects on VSM contraction; however, several novel ZIPK regulators have been revealed in recent years. Notably, the prostate apoptosis response-4 (Par-4) protein is suggested to facilitate VSM contraction by acting as a cytoskeletal scaffold for ZIPK (Vetterkind et al., 2010; Vetterkind and Morgan, 2009). While the upstream activating pathways for ZIPK have yet to be resolved, evidence suggests that the kinase can be activated in VSM in response to external stimuli (Graves et al., 2005; Hagerty et al., 2007; MacDonald et al., 2001a) and ZIPK can be

phosphorylated by Rho-associated coiled coil-containing kinase (ROCK) (Hagerty et al., 2007).

Pharmacological agents can provide powerful insight into signaling mechanisms if used appropriately. Four independent groups have recently reported the development of novel ZIPK inhibitory compounds: (i) Velentza *et al.* reported the first small molecule DAPK inhibitor, an alkylated 3-amino-6-phenylpyridazine (Velentza et al., 2003); (ii) Okamoto *et al*. used structure-based, virtual screening to identify DAPK1 and ZIPK inhibitors with a 2-phenyl-4-(3-pyridinylmethylene)-5(4*H*)-oxazolone core (Okamoto et al., 2009; Okamoto et al., 2010); (iii) Huber *et al.* identified inhibitory oxo-β-carboline compounds that do not rely on canonical ATP competition (Huber et al., 2012); and (iv) Carlson *et al*. used a chemoproteomic FLECS screening to identify an aryl-thiopyrazolo[3,4-*d*]pyrimidinone (i.e., HS38) that competitively inhibits ZIPK (Carlson et al., 2013). HS38 displays similar or greater potency for ZIPK and has fewer off-target liabilities than other published ZIPK inhibitors (Carlson et al., 2013). The availability of a cell-permeable, potent and selective inhibitor provides a novel opportunity to examine aspects of ZIPK signaling in VSM that were previously not attainable, and we have used HS38 to study the mechanistic role of ZIPK in Ca^{2+} sensitization of VSM.

Materials and Methods

Materials- 2-((1-(3-chlorophenyl)-4-oxo-4,5-dihydro-1H-pyrazolo [3,4-*d*]-pyrimidin-6-yl)thio)propanamide (HS38) and 1-(3-chlorophenyl)-6-((2-hydroxyethyl)thio)-1,5-dihydro-4*H*-pyrazolo[3,4-*d*]pyrimidin-4-one (HS43) were synthesized in the Haystead

Molecular Pharmacology Fast Forward. Published on October 13, 2015 as DOI: 10.1124/mol.115.100529
This article has not been copyedited and formatted. The final version may differ from this version.

laboratory at Duke University as previously described (Carlson et al., 2013). Only trace impurities were identified (< 1% by LC coupled to mass spectrometry). Calyculin A (CLa), angiotensin II (AngII), endothelin-1 (ET-1) and U46619 were purchased from EMD Millipore (Billerica, MA) and phenylephrine (PE) was obtained from Sigma Chemical Co. (St. Louis, MO). The Supersignal West Femto Chemiluminescence Kit was from GE Healthcare (Piscataway, NJ). Antibodies specific for CPI-17 and Par-4 were purchased from EMD Millipore. Phosphospecific antibodies for MYPT1 phosphorylated at Thr697 or Thr855 were purchased from EMD Millipore. Phos-Tag-acrylamide was purchased from NARD Chemicals Inc. (Kobe City, Japan). Purified ROCK2 was purchased from SignalChem (Richmond, BC). LC_{20} (Hathaway and Haeberle, 1983) and MLCK (Ngai et al., 1984) proteins were purified from chicken gizzard as previously described. All other chemicals were reagent grade and were obtained from Sigma Chemical Co. or VWR (Mississauga, ON, Canada).

In Vitro Kinase Assays-ROCK2 and MLCK activities were assayed at 25 °C with LC_{20} protein substrate under standard conditions (25 mM HEPES, pH 7.4, 1 mM $MgCl_2$, 0.2 mM ATP, and 2 μCi of [γ-^{32}P]-ATP). Reactions were initiated by the addition of ATP and terminated by spotting the mixture onto phosphocellulose P81 paper. After extensive washing with 20 mM H_3PO_4, ^{32}P incorporation was determined by scintillation counting.

Tissue Preparation and Force Measurements- Caudal arteries were removed from male Sprague-Dawley rats (~300 g) that had been anesthetized and euthanized according to protocols approved by the University of Calgary Animal Care and Use Committee. The arteries were cleaned of excess adventitia, denuded of endothelium, and cut into helical strips (1.5 mm x 6 mm). Muscle strips were mounted on a Grass isometric force

Molecular Pharmacology Fast Forward. Published on October 13, 2015 as DOI: 10.1124/mol.115.100529
This article has not been copyedited and formatted. The final version may differ from this version.

transducer (FT03C) and force was recorded as previously described (Moffat et al., 2011). Intact tissues were treated with CLa (0.5 μM) in HEPES-buffered Tyrode's solution (H-T buffer) contained 137 mM NaCl, 2.7 mM KCl, 1 mM $MgCl_2$, 1.8 mM $CaCl_2$, 5.6 mM glucose, 10 mM HEPES, pH 7.4. Isolated smooth muscle strips, pre-incubated with HS38 or vehicle (DMSO), were also stimulated with the following contractile agonists in H-T buffer: the thromboxane A_2 mimetic U46619, ET-1, AngII, PE or KCl (87 mM KCl replaced 87 mM NaCl in H-T buffer). At selected times, muscle strips were flash-frozen in 10% (w/v) TCA, 10 mM DTT in acetone followed by 3 x 10 s washes in 10 mM DTT in acetone. Tissues were then lyophilized overnight prior to protein extraction.

Analysis of LC_{20}, MYPT1, Par-4 and CPI-17 Phosphorylation-Protein was extracted from each lyophilized tissue in 1 ml of SDS-gel sample buffer with constant shaking for 16 h at 4 ^{o}C. Tissue proteins were resolved by Phos-Tag SDS-PAGE and western blotting for the measurement of LC_{20}, Par-4 and CPI-17 phosphorylation (Ihara et al., 2015; Moffat et al., 2011; Takeya et al., 2008), and by SDS-PAGE and western blotting with phosphospecific antibodies for MYPT1 phosphorylation (Grassie et al., 2012; Mills et al., 2015). For CPI-17, 12.5% acrylamide and 30 μM Phos-Tag reagent were used, proteins were transferred to polyvinylidene difluoride (PVDF; Roche) overnight at 25 V and 4 ^{o}C in 10 mM CAPS, pH 11, 10% methanol. For LC_{20}, 12.5% acrylamide and 50 μM Phos-Tag reagent were used; proteins were transferred to PVDF overnight at 27 V and 4 ^{o}C in 25 mM Tris-HCl, pH 7.5, 192 mM glycine, 10% (v/v) methanol. Following transfer, proteins were fixed on the membrane by incubation for 20 min with 0.5% glutaraldehyde in phosphate-buffered saline and nonspecific binding sites were blocked with 5% (w/v) non-fat dry milk (for LC_{20}) or with 2% ECL blocking reagent (for CPI-17) in TBST for 1

Molecular Pharmacology Fast Forward. Published on October 13, 2015 as DOI: 10.1124/mol.115.100529
This article has not been copyedited and formatted. The final version may differ from this version.

h at room temperature. Membranes were incubated overnight with anti-LC_{20} (Santa Cruz Biotechnology, Santa Cruz, CA, catalog number sc-15370) at 1:500 dilution in 1% (w/v) non-fat dry milk, then for 1 h with HRP-conjugated secondary antibody (Chemicon, Temecula, CA) at 1:10,000 dilution, or for 2 h with anti-CPI-17 (EMD Millipore, catalog number 07-344) at 1:5,000 dilution, then for 1 h with biotin-labeled secondary antibody (EMD Millipore, catalog number AP132B) at 1:10,000 dilution, followed by streptavidin-HRP (Pierce Chemical Co., Rockford, IL, catalog number PI-21126) at 1:5,000 dilution for 30 min. For Par-4, 7.5% acrylamide and 60 μM Phos-tag reagent were used, proteins were transferred to 0.2-μm nitrocellulose membrane overnight at 28 V and 4 ^{o}C in 25 mM Tris-HCl, pH 7.5, 192 mM glycine, 10% (v/v) methanol, blocked with 5% skim milk in TBST for 1 h at room temperature and incubated with anti-Par-4 (Abcam, catalog number 2853-1) at 1:5,000 dilution for 2 h at room temperature, followed by anti-rabbit IgG (EMD Millipore, catalog number AP132P) at 1:5,000 dilution for 1 h at room temperature. For analysis of MYPT1 phosphorylation, tissue homogenates were resolved by 10% SDS-PAGE and transferred to nitrocellulose membranes. Membranes were incubated with anti-[phospho-Thr697]-MYPT1 (Millipore, catalog number ABS45) at 1:3,500 dilution or anti-[phospho-Thr855]-MYPT1 (Millipore, catalog number 36-003) at 1:3,000 dilution, and then for 1 h with HRP-conjugated secondary antibody (EMD Millipore, catalog number AP132P; 1:5,000 dilution). Smooth muscle α-actin was used as a loading control with antibodies from Cytoskeleton Inc. (Denver, CO, catalog number AAN01; 1:5,000 dilution). All western blots were visualized with West Femto Enhanced Chemiluminescence (ECL) reagent using a LAS4000 Imaging Station (GE Healthcare), ensuring that the representative

Molecular Pharmacology Fast Forward. Published on October 13, 2015 as DOI: 10.1124/mol.115.100529
This article has not been copyedited and formatted. The final version may differ from this version.

signal occurred in the linear range. Quantification was performed by densitometry with ImageQuant TL software (GE Healthcare). LC_{20} phosphorylation stoichiometry was calculated as follows: mol P_i/mol LC_{20} = [LC_{20}-1P + (2 x LC_{20}-2P) + (3 x LC_{20}-3P)]/[LC_{20}-0P + LC_{20}-1P + LC_{20}-2P + LC_{20}-3P].

Data Analysis- Values are presented as the mean ± S.E.M., with *n* indicating the number of animals (tissue experiments). Data were analyzed by Student's *t* test (two-tailed). For comparison of multiple groups, significance was determined by two-way analysis of variance with Dunnett's *post hoc* test. Differences were considered to be statistically significant when $p < 0.05$.

Results

The pyrazolo[3,4-*d*]pyrimidinone derivative HS38 was previously characterized as a potent inhibitor of ZIPK (Carlson et al., 2013). HS38 acts as a competitive inhibitor with respect to ATP and was reported to be most potent toward ZIPK (K_d 280 nM), DAPK1 (K_d 300 nM) and PIM3 (K_d 810 nM), 10-fold less potent against IRAK4 and PIM1, 100-fold less potent against PIM2 and MLCK, and inactive against ROCK2. Indeed, more detailed *in vitro* kinetic assessments of the inhibitory potential of HS38 toward ROCK2 and MLCK indicated that it has no significant effect on these contractile kinases at concentrations up to 100 μM (Fig. 1A and B). We employed isolated rat caudal arterial smooth muscle strips as a model VSM tissue and assessed the concentration and time dependence of HS38 effects on contractile responses. Muscle strips were incubated in Ca^{2+}-containing HEPES buffer with HS38 or vehicle prior to addition of the type 1 and

Molecular Pharmacology Fast Forward. Published on October 13, 2015 as DOI: 10.1124/mol.115.100529
This article has not been copyedited and formatted. The final version may differ from this version.

2A phosphatase inhibitor CLa, which, by inhibiting endogenous MLCP activity, unmasks basal Ca^{2+}-independent LC_{20} kinase activities to induce a slow, sustained contraction (Sutherland and Walsh, 2012; Wilson et al., 2005b). HS38 appeared to attenuate the velocity of the contractile responses, whereas the steady-state level of force induced by CLa was unaffected by ZIPK inhibition (Fig. 1C-D), a result that was previously demonstrated (Carlson et al., 2013). As shown in Table 1, the mean steady-state force induced by CLa was ~160% of that induced by KCl (87 mM) and was unaffected by pre-treatment with HS38. We did observe variability in the steady-state force levels induced by calyculin A, relative to KCl, from tissue to tissue, as indicated by the S.D. values in parentheses in Table 1. This variability can be attributed to variations in the dimensions of the muscle strips. The latency period, i.e. the time from addition of CLa to the onset of contraction, and the half-time from the initiation of contraction to the plateau of the contractile response, in addition to the $t_{1/2}$ values (the half-time from addition of CLa to the plateau of the contractile response) were all significantly increased in the presence of HS38 (Table 1). Significant increases in $t_{1/2}$ were observed at concentrations of HS38 $\geq$ 10 μM, and maximal effects (~2-fold increase in $t_{1/2}$) were observed at HS38 concentrations $\geq$ 50 μM (Fig. 1E). On the other hand, increasing HS38 concentration did not affect the maximal developed force (Fig. 1F).

We addressed the possibility that HS38 may influence $[Ca^{2+}]_i$ by examining Fluo-4-loaded, de-endothelialized rat caudal artery strips. As shown in Supplemental Figure 1, HS38 had no effect on the depolarization-induced Ca^{2+} transient.

Finally, the effects of HS38 on the contractile response to CLa were found to be reversible. Treatment of de-endothelialized rat caudal arterial smooth muscle strips with

Molecular Pharmacology Fast Forward. Published on October 13, 2015 as DOI: 10.1124/mol.115.100529
This article has not been copyedited and formatted. The final version may differ from this version.

HS38 (50 μM for 30 min or 3 h), followed by washout, restored $t_{1/2}$ values of CLa-induced contraction to that observed with no prior exposure to HS38 (Fig. 2A-B).

The effect of HS38 on LC_{20} phosphorylation was assessed to determine if inhibition of LC_{20} phosphorylation underlies the HS38-induced reduction of the rate of CLa-induced contraction. HS38 suppressed CLa-induced LC_{20} phosphorylation in a concentration-dependent manner, with significant inhibition observed at concentrations of HS38 $\geq$ 25 μM (Fig. 3A). The inhibitory effect of HS38 on LC_{20} phosphorylation was confirmed by analysis of the time-course of CLa-induced phosphorylation of LC_{20} in the absence and presence of HS38 (100 μM) (Fig. 3B-D). The fact that LC_{20} phosphorylation was not abolished by HS38 is consistent with the unmasking of the activities of other kinases, such as integrin-linked kinase (ILK) (Wilson et al., 2005b), upon CLa treatment.

ZIPK was originally isolated from smooth muscle as an MLCP-associated kinase (MacDonald et al., 2001a), and studies have demonstrated its ability to phosphorylate MYPT1 (the regulatory, myosin-targeting subunit of the phosphatase) *in vitro* and *in situ* (Endo et al., 2004; MacDonald et al., 2001a; Moffat et al., 2011). A basal level of phosphorylation was observed at both Thr inhibitory sites, Thr697 (Fig. 4A) and Thr855 (Fig. 4D). Exposure of smooth muscle strips to HS38 reduced the basal phosphorylation observed under resting conditions (time zero) at both sites (Fig. 4B and 4E), so there is likely some basal ZIPK activity (or other kinase activity influenced by ZIPK) that contributes to MYPT1 phosphorylation under rest/basal conditions. It is noticeable that the electrophoretic mobility of phospho-MYPT1-immunoreactive bands decreased with time of exposure to CLa, suggesting that MYPT1 is hyperphosphorylated at multiple sites upon phosphatase inhibition. After normalizing the MYPT1 phosphorylation immuno-

Molecular Pharmacology Fast Forward. Published on October 13, 2015 as DOI: 10.1124/mol.115.100529
This article has not been copyedited and formatted. The final version may differ from this version.

signals against α-actin to account for loading variability, we were also able to report the change in phosphorylation signal relative to the initial basal/resting level. The application of HS38 resulted in an unexpected accumulation of MYPT1 phosphorylation at both Thr697 (Fig. 4C) and Thr855 (Fig. 4F) when compared with CLa stimulation alone. We have previously observed increased MYPT1 phosphorylation upon blockade of ZIPK signaling in rat caudal artery (Moffat et al., 2011); this observation was made during loading of recombinant, kinase-dead ZIPK protein into Triton-skinned muscle strips with MLCP inhibition by microcystin-LR. We have interpreted this phenomenon to be a result of coincident unmasking of kinase activities with MLCP inhibitors and suppression of ZIPK activity. The resulting changes associated with the contractile architecture may allow the phosphorylation sites of MYPT1 to become more accessible, as theorized by Vetterkind and colleagues (Vetterkind et al., 2010; Vetterkind and Morgan, 2009).

The *in vitro* phosphorylation of CPI-17 by ZIPK has been reported previously (MacDonald et al., 2001b). Treatment of caudal arterial smooth muscle strips with CLa resulted in slow stoichiometric phosphorylation of CPI-17 at several sites, as shown by Phos-Tag SDS-PAGE (Fig. 5A). In this case, HS38 had no effect on CLa-induced CPI-17 phosphorylation stoichiometry (Fig. 5B).

The prostate apoptosis response-4 (Par-4, 36 kDa) protein is expressed in differentiated VSM cells (Vetterkind et al., 2010; Vetterkind and Morgan, 2009) and is suggested to facilitate contraction by acting as a cytoskeletal scaffold for ZIPK. Therefore, we investigated the effects of HS38 on Par-4 phosphorylation in response to CLa stimulation of caudal arterial smooth muscle and observed that CLa treatment induced the phosphorylation of Par-4 at multiple sites (Fig. 6A). Eight distinct

Molecular Pharmacology Fast Forward. Published on October 13, 2015 as DOI: 10.1124/mol.115.100529
This article has not been copyedited and formatted. The final version may differ from this version.

phosphorylated species were detected by Phos-Tag SDS-PAGE, but HS38 (100 μM) had no effect on the rate or maximal stoichiometry of Par-4 phosphorylation (Fig. 6A-C).

Although HS38 has been described as a potent and selective ZIPK inhibitor, it does retain some off-target activity towards members of the proviral integrations of Moloney virus (PIM) kinase family (Carlson et al., 2013), which have roles in cell growth, proliferation, apoptosis and regulation of signal transduction cascades (Alvarado et al., 2012). Currently, there are no reports of PIM kinases contributing to smooth muscle contractility; however, we felt it prudent to assess whether any of the observed effects of HS38 on VSM contractility could be attributed to inhibition of PIM kinases. In this regard, a structural ortholog (HS43) was developed from the HS38 backbone (Carlson et al., 2013). This compound retains selective potency toward PIM3 with minimal activity towards ZIPK. The HS43 compound was applied to de-endothelialized rat caudal arterial strips, and the contractile responses to CLa were monitored (Fig. 7A). No effect was observed for HS43 on the velocity of contraction (Fig. 7B) or maximal force (Fig. 7C). Finally, CLa-induced phosphorylations of LC_{20} (Fig. 7D), Par-4 (Fig. 7E and F) and MYPT1 (Fig. 7G and H) were also unaffected by inhibition of PIM3 kinase activity with HS43.

The development of a potent and selective ZIPK inhibitor provides the opportunity to examine upstream receptor-signaling modules that are linked to ZIPK-dependent contractile responses. Isolated rat caudal arterial smooth muscle strips were again employed since receptor-mediated contractile responses have been extensively explored in this VSM tissue (Grassie et al., 2012; Mita et al., 2002; Weber et al., 1999; Wilson et al., 2005a; Wilson et al., 2005b). The typical contractile response of this tissue to agonist

Molecular Pharmacology Fast Forward. Published on October 13, 2015 as DOI: 10.1124/mol.115.100529
This article has not been copyedited and formatted. The final version may differ from this version.

stimulation can be divided into an initial, rapid phasic response and a sustained, steady-state tonic response. The effects of HS38 pre-treatment on the contractile responses to a range of agonists were investigated (Fig. 8A). PE (1 μM), ET-1 (0.1 μM) and high-[K^+] extracellular solution (87 mM KCl) induced robust contractile responses. Other stimuli (the thromboxane A_2 mimetic U46619 (1 μM) and AngII (0.1 μM)) elicited contractile responses of reduced magnitude. Both the force developed in the early phasic response (i.e., peak tension at 2-5 min) and the sustained tonic response (i.e., sustained force at 15 min) to all agonists were significantly inhibited by pre-treatment with HS38 (Fig. 8B and C).

Agonist-induced contractions were associated with LC_{20} phosphorylation exclusively at a single site (Fig. 9A), previously identified as Ser19, as expected (e.g. (Sutherland and Walsh, 2012)). LC_{20} phosphorylation was significantly increased at the peak of the contractile response to PE, U46619, KCl, and ET-1 (Fig. 9A and B). All of these agonist-induced increases in LC_{20} phosphorylation were abolished or significantly reduced by pre-incubation of the tissue with HS38 (Fig. 9A and B). In addition, the data showed no change in LC_{20} phosphorylation following stimulation with AngII, but a significant decrease was observed during AngII treatment in the presence of HS38. The effect of HS38 on agonist-induced phosphorylation of MYPT1 at Thr697 and Thr855 was also investigated. PE-induced Thr697 phosphorylation was reduced by ~50% by HS38. Thr855 phosphorylation induced by PE, KCl and ET-1 was also suppressed by ~50% by HS38 (Figure 9C and D). Finally, agonist-induced phosphorylation of CPI-17 was assessed in the absence or presence of HS38 (Fig. 9E and F). Stimulation with all agonists (i.e., PE, U46619, KCl, AngII and ET-1) enhanced CPI-17 phosphorylation

Molecular Pharmacology Fast Forward. Published on October 13, 2015 as DOI: 10.1124/mol.115.100529
This article has not been copyedited and formatted. The final version may differ from this version.

relative to control, and HS38 pre-treatment significantly suppressed the increase in CPI-17 phosphorylation induced by PE, AngII and ET-1. In contrast, HS38 treatment had no influence on CPI-17 phosphorylation induced with U46619 or KCl.

Discussion

The inhibitory potential of the HS38 molecule against ZIPK was first defined in 2013, and some basic assessments of its effects on smooth muscle cells and tissues were completed to support its potential utility as a lead scaffold for future development and application to cardiovascular systems (Carlson et al., 2013). In this regard, HS38 could alter *ex vivo* contractile force development of various smooth muscles isolated from rabbit, rat and mouse. HS38 could attenuate LC_{20} phosphorylation in human coronary and aorta vascular smooth muscle cells in response to stimulation with serum and sphingosine-1-phosphate, respectively. In addition, HS38 suppressed Ca^{2+}-independent force production and LC_{20} phosphorylation in permeabilized rabbit ileum treated with the MLCP inhibitor microcystin-LR. The lag time to the onset of force was increased, and the rate of force development was decreased. Additional pilot studies with rat caudal artery revealed the ability of HS38 to attenuate LC_{20} phosphorylation and contractile force development. The initial findings supported a novel hypothesis that the ability of ZIPK to regulate the Ca^{2+} sensitization of smooth muscle contraction is conserved across species and smooth muscle tissues. Collectively, these results provided conclusive support for the role of ZIPK in the Ca^{2+}-independent phosphorylation of LC_{20}; however, the role of the kinase in agonist-dependent contraction remained largely unexamined. Herein, we were able to employ HS38 to comprehensively define the mechanistic role for

Molecular Pharmacology Fast Forward. Published on October 13, 2015 as DOI: 10.1124/mol.115.100529
This article has not been copyedited and formatted. The final version may differ from this version.

ZIPK in the Ca^{2+}-sensitizing pathways that regulate VSM contractile tone.

Intriguing differences were observed for the ZIPK-dependent contractile responses of caudal arterial strips, depending on the mode of activation. Treatment with CLa to inhibit type 1 and 2A phosphatases (including MLCP, a type 1 phosphatase), and thereby unmask endogenous kinase activities, yielded robust LC_{20} mono- and diphosphorylation that was sensitive to ZIPK inhibition by HS38; however, the suppression of ZIPK activity did not relieve MLCP inhibition, i.e., significant amounts of CLa-induced MYPT1 phosphorylation at Thr697 and Thr855 were still observed in the presence of HS38. In contrast, agonist-induced stimulation of GPCRs and activation of downstream Ca^{2+} sensitization pathways elicited notable effects on phosphorylation of MYPT1 and CPI-17, as well as LC_{20}. Based on these distinct responses, we speculate that two functional pools of ZIPK exist in this VSM tissue: (i) a constitutively-active ZIPK associated with the myosin II compartment, and (ii) an inactive ZIPK pool that is intimately associated with MLCP and its regulatory apparatus (e.g., Par-4, CPI-17 and the myosin phosphatase-Rho interacting protein, M-RIP). The first pool of ZIPK would be available to act as a Ca^{2+}-independent MLCK and evoke LC_{20} diphosphorylation upon MLCP inhibition. The second pool of ZIPK would require activation by upstream signaling molecules to increase ZIPK activity and induce MYPT1 and/or CPI-17 phosphorylation, thereby decreasing MLCP activity and increasing LC_{20} phosphorylation at Ser19 by MLCK.

Various reports in the literature have described distinct forms of ZIPK in VSM. Independent methods have been used to separately purify ZIPK as an MLCP-associated kinase (MacDonald et al., 2001a) and a Ca^{2+}-independent LC_{20} kinase (Borman et al., 2002), both of which were 32 kDa proteins. These two proteins were shown to be ZIPK

Molecular Pharmacology Fast Forward. Published on October 13, 2015 as DOI: 10.1124/mol.115.100529
This article has not been copyedited and formatted. The final version may differ from this version.

by immunoblotting and protein sequencing. However, other researchers have detected the full-length 54 kDa protein in VSM tissues (Endo et al., 2004; Niiro and Ikebe, 2001; Vetterkind and Morgan, 2009). The presence of a leucine zipper (LZ) motif in the full-length ZIPK sequence, and in certain MYPT1 isoforms, could provide an effective mechanism for linking the two proteins. The presence of the LZ, however, does not enhance ZIPK activity towards MYPT1 (Niiro and Ikebe, 2001). Furthermore, the presence of a LZ does not appear to be necessary for the localization of ZIPK to MLCP as demonstrated by our original isolation of the truncated 32 kDa kinase with MLCP activity (MacDonald et al., 2001a), our co-immunoprecipitation of the 32 kDa isoform of ZIPK from bladder smooth muscle with MYPT1 (MacDonald et al., 2001a), and later work showing that both full-length ZIPK and ZIPK lacking the LZ can interact with MYPT1 (Endo et al., 2004; Takamoto et al., 2006). However, the LZ does appear to have some role in controlling both the activity and the cellular localization of ZIPK. Mutation of the LZ resulted in a decreased ability of ZIPK to induce cell death when over-expressed in NIH3T3 cells (Kawai et al., 1998) and in a predominantly nuclear localization of the kinase (Graves et al., 2005). Additional investigations are required to explore how ZIPK signaling is compartmentalized within VSM to independently regulate LC_{20} and MYPT1/CPI-17 phosphorylation.

Previous evidence suggested that ZIPK could be activated in VSM in response to agonist stimulation (MacDonald et al., 2001a); however, the upstream signaling architecture for the regulation of ZIPK activity in VSM (e.g., GPCRs and activating kinase pathways) has not been interrogated in detail. Herein, we provide the first examination of GPCR-mediated modulation of ZIPK contractile responses. The

Molecular Pharmacology Fast Forward. Published on October 13, 2015 as DOI: 10.1124/mol.115.100529
This article has not been copyedited and formatted. The final version may differ from this version.

inhibition of ZIPK by HS38 significantly influenced the VSM contractile responses to a variety of physiological agonists, acting via their cognate receptors, including phenylephrine, U46619, AngII and ET-1. Canonical pharmacomechanical coupling of agonists and contractile force development involves changes in $[Ca^{2+}]_i$ as well as activation of Ca^{2+}-sensitizing signal transduction pathways (Wettschureck and Offermanns, 2005; Wynne et al., 2009). The former may involve $G\alpha_{q/11}$-mediated PLCβ activation with downstream diacylglycerol and inositol 1,4,5-trisphosphate effects on internal Ca^{2+} stores. The latter may involve $G\alpha_{q/11}$- or $G\alpha_{12/13}$-mediated activation of PKC and/or RhoA/ROCK. Given the fact that these agonist/receptor pairs activate similar downstream signaling pathways in VSM, it is clear why inhibition of ZIPK activity by HS38 attenuated the contractile responses to all these agonists.

We addressed the possibility that HS38 influenced $[Ca^{2+}]_i$ (Supplemental Figure 1) since Ca^{2+}-dependent MLCK activity is absolutely required for both the phasic and tonic components of the contractile responses to agonists and depolarization. During the sustained contractile response, when $[Ca^{2+}]_i$ has declined, the MLCK activity is low relative to its activation during the phasic response and, without inhibition of MLCP activity, will be insufficient to maintain LC_{20} phosphorylation and force (Mita et al., 1997; Mita et al., 2002). Given that HS38 had no effect on depolarization-induced Ca^{2+} signaling or MLCK activity but inhibited both contraction and MYPT1 phosphorylation (which has been implicated in the mechanism of Ca^{2+}sensitization), it is reasonable to conclude that ZIPK is involved in Ca^{2+} sensitization but not Ca^{2+}-induced contraction induced by membrane depolarization. Inhibition of agonist-induced contraction by HS38

Molecular Pharmacology Fast Forward. Published on October 13, 2015 as DOI: 10.1124/mol.115.100529
This article has not been copyedited and formatted. The final version may differ from this version.

also involves Ca^{2+} desensitization, so we cannot rule out an additional inhibitory effect on Ca^{2+} signaling.

There is good evidence that ZIPK is regulated by phosphorylation at multiple sites by ROCK1 (Hagerty et al., 2007) and DAPK1 (Shani et al., 2004). The involvement of RhoA/ROCK in Ca^{2+} sensitization of VSM contraction has been unequivocally demonstrated. In this regard, ROCK can be activated in a variety of smooth muscle types in response to a large number of different contractile agonists (Puetz et al., 2009). The activation of RhoA/ROCK by $G\alpha_{12/13}$ is mediated by guanine nucleotide exchange factors (GEFs, including p115-RhoGEF, PDZ-RhoGEF and LARG) and can be stimulated by administration of AngII, ET-1 or U46619 (Amin et al., 2013; Puetz et al., 2009; Wettschureck and Offermanns, 2005). RhoA/ROCK activation through $G\alpha_{q/11}$ can result in contractile responses to PE; however, the functional linkages are incompletely understood (Puetz et al., 2009; Wettschureck and Offermanns, 2005). Moreover, KCl-induced membrane depolarization also elicits sustained contraction of VSM via activation of the RhoA/ROCK pathway (Mills et al., 2015; Mita et al., 2013; Mita et al., 2002; Sakamoto et al., 2003; Sakurada et al., 2003; Urban et al., 2003). The effects of inhibition of ZIPK during agonist-dependent contractions of caudal arterial smooth muscle suggest that the kinase lies downstream of GPCRs that signal through both $G\alpha_{12/13}$ and $G\alpha_{q/11}$ (Fig. 10). There may be integration of ROCK and ZIPK downstream of $G\alpha_{12/13}$ to regulate Ca^{2+} sensitization processes and force generation since ROCK has been demonstrated to directly activate ZIPK by phosphorylating ZIPK at Thr265 and Thr299 (Hagerty et al., 2007). Phosphorylation at Thr265 activates ZIPK whereas phosphorylation at Thr299 regulates its intracellular localization by preventing its

Molecular Pharmacology Fast Forward. Published on October 13, 2015 as DOI: 10.1124/mol.115.100529
This article has not been copyedited and formatted. The final version may differ from this version.

translocation from the cytosol to the nucleus. *In vitro*, co-expression of ZIPK with ROCK also changes the focused stress fiber pattern of cells to a phenotype of parallel stress fibers. Although these data suggest ROCK may regulate ZIPK in non-muscle cells, the finding has yet to be confirmed in VSM tissue.

Alternatively, it is possible that ZIPK is primarily integrated with $G\alpha_{q/11}$-PLCβ and PKC signaling to regulate Ca^{2+} sensitization. ZIPK can phosphorylate CPI-17 at the phosphatase-inhibitory Thr38 site *in vitro* (MacDonald et al., 2001b). So, it is possible that PKC may activate ZIPK or *vice versa*. A recent report by Xu and colleagues revealed that PKC/CPI-17 and ZIPK might participate to regulate the Ca^{2+} sensitivity of mesenteric arterial constriction after hemorrhagic shock (Xu et al., 2010). These authors suggested an intermediary role for ZIPK, whereby it acts as a bridge between PKC at the plasma membrane and MLCP at the contractile apparatus. Therefore, additional *in vivo* evaluation of ZIPK, especially in relation to the RhoA/ROCK and PKC pathways, will be important to further our understanding of signal transduction cross-talk of Ca^{2+} sensitizing pathways and perhaps also lead to better treatments for cardiovascular diseases.

Authorship Contributions

Participated in research design: MacDonald, Haystead, Swärd, and Walsh

Conducted experiments: Sutherland, Bhaidani, Swärd, and Al-Ghabkari

Contributed new reagents or analytic tools: Carlson and Haystead

Performed data analysis: MacDonald, Sutherland, Swärd, and Walsh

Wrote or contributed to writing of the manuscript: MacDonald and Walsh

References

Alvarado Y, Giles FJ and Swords RT (2012) The PIM kinases in hematological cancers. *Expert Rev Hematol* 5(1): 81-96.

Amin E, Dubey BN, Zhang SC, Gremer L, Dvorsky R, Moll JM, Taha MS, Nagel-Steger L, Piekorz RP, Somlyo AV and Ahmadian MR (2013) Rho-kinase: regulation, (dys)function, and inhibition. *Biol Chem* 394(11): 1399-1410.

Borman MA, MacDonald JA, Muranyi A, Hartshorne DJ and Haystead TA (2002) Smooth muscle myosin phosphatase-associated kinase induces Ca2+ sensitization via myosin phosphatase inhibition. *J Biol Chem* 277(26): 23441-23446.

Carlson DA, Franke AS, Weitzel DH, Speer BL, Hughes PF, Hagerty L, Fortner CN, Veal JM, Barta TE, Zieba BJ, Somlyo AV, Sutherland C, Deng JT, Walsh MP, MacDonald JA and Haystead TA (2013) Fluorescence Linked Enzyme Chemoproteomic Strategy for Discovery of a Potent and Selective DAPK1 and ZIPK Inhibitor. *ACS Chem Biol* 8(12):1648-1659.

Endo A, Surks HK, Mochizuki S, Mochizuki N and Mendelsohn ME (2004) Identification and characterization of zipper-interacting protein kinase as the unique vascular smooth muscle myosin phosphatase-associated kinase. *J Biol Chem* 279(40): 42055-42061.

Georgescu A, Alexandru N, Nemecz M, Titorencu I and Popov D (2011) Enoxaparin reduces adrenergic contraction of resistance arterioles in aging and in aging associated with diabetes via engagement of MAP kinase pathway. *Blood Coagul Fibrinolysis* 22(4): 310-316.

Grassie ME, Sutherland C, Ulke-Lemee A, Chappellaz M, Kiss E, Walsh MP and MacDonald JA (2012) Cross-talk between Rho-associated kinase and cyclic nucleotide-dependent kinase signaling pathways in the regulation of smooth muscle myosin light chain phosphatase. *J Biol Chem* 287(43): 36356-36369.

Graves PR, Winkfield KM and Haystead TA (2005) Regulation of zipper-interacting protein kinase activity in vitro and in vivo by multisite phosphorylation. *J Biol Chem* 280(10): 9363-9374.

Hagerty L, Weitzel DH, Chambers J, Fortner CN, Brush MH, Loiselle D, Hosoya H and Haystead TA (2007) ROCK1 phosphorylates and activates zipper-interacting protein kinase. *J Biol Chem* 282(7): 4884-4893.

Hathaway DR and Haeberle JR (1983) Selective purification of the 20,000-Da light chains of smooth muscle myosin. *Anal Biochem* 135(1): 37-43.

Haystead TA (2005) ZIP kinase, a key regulator of myosin protein phosphatase 1. *Cell Signal* 17(11): 1313-1322.

Hirano K (2007) Current topics in the regulatory mechanism underlying the Ca2+ sensitization of the contractile apparatus in vascular smooth muscle. *J Pharmacol Sci* 104(2): 109-115.

Huber K, Brault L, Fedorov O, Gasser C, Filippakopoulos P, Bullock AN, Fabbro D, Trappe J, Schwaller J, Knapp S and Bracher F (2012) 7,8-dichloro-1-oxo-beta-carbolines as a versatile scaffold for the development of potent and selective kinase inhibitors with unusual binding modes. *J Med Chem* 55(1): 403-413.

Ihara E, Edwards E, Borman MA, Wilson DP, Walsh MP and MacDonald JA (2007) Inhibition of zipper-interacting protein kinase function in smooth muscle by a

myosin light chain kinase pseudosubstrate peptide. *Am J Physiol Cell Physiol* 292(5): C1951-1959.

Ihara E and MacDonald JA (2007) The regulation of smooth muscle contractility by zipper-interacting protein kinase. *Can J Physiol Pharmacol* 85(1): 79-87.

Ihara E, Yu Q, Chappellaz M and MacDonald JA (2015) ERK and p38MAPK pathways regulate myosin light chain phosphatase and contribute to Ca2+ sensitization of intestinal smooth muscle contraction. *Neurogastroenterol Motil* 27(1): 135-146.

Katsumata N, Shimokawa H, Seto M, Kozai T, Yamawaki T, Kuwata K, Egashira K, Ikegaki I, Asano T, Sasaki Y and Takeshita A (1997) Enhanced myosin light chain phosphorylations as a central mechanism for coronary artery spasm in a swine model with interleukin-1beta. *Circulation* 96(12): 4357-4363.

Kawai T, Matsumoto M, Takeda K, Sanjo H and Akira S (1998) ZIP kinase, a novel serine/threonine kinase which mediates apoptosis. *Mol Cell Biol* 18(3): 1642-1651.

Kim HR, Appel S, Vetterkind S, Gangopadhyay SS and Morgan KG (2008) Smooth muscle signalling pathways in health and disease. *J Cell Mol Med* 12(6A): 2165-2180.

MacDonald JA, Borman MA, Muranyi A, Somlyo AV, Hartshorne DJ and Haystead TA (2001a) Identification of the endogenous smooth muscle myosin phosphatase-associated kinase. *Proc Natl Acad Sci U S A* 98(5): 2419-2424.

MacDonald JA, Eto M, Borman MA, Brautigan DL and Haystead TA (2001b) Dual Ser and Thr phosphorylation of CPI-17, an inhibitor of myosin phosphatase, by MYPT-associated kinase. *FEBS Lett* 493(2-3): 91-94.

Masumoto A, Mohri M, Shimokawa H, Urakami L, Usui M and Takeshita A (2002) Suppression of coronary artery spasm by the Rho-kinase inhibitor fasudil in patients with vasospastic angina. *Circulation* 105(13): 1545-1547.

Mills RD, Mita M, Nakagawa J, Shoji M, Sutherland C and Walsh MP (2015) A role for the tyrosine kinase Pyk2 in depolarization-induced contraction of vascular smooth muscle. *J Biol Chem* 290(14): 8677-8692.

Mita M and Walsh MP (1997) Alpha1-adrenoceptor-mediated phosphorylation of myosin in rat-tail arterial smooth muscle. *Biochem J* 327(Pt 3): 669-674.

Mita M, Tanaka H, Yanagihara H, Nakagawa J, Hishinuma S, Sutherland C, Walsh MP and Shoji M (2013) Membrane depolarization-induced RhoA/Rho-associated kinase activation and sustained contraction of rat caudal arterial smooth muscle involves genistein-sensitive tyrosine phosphorylation. *J Smooth Muscle Res* 49: 26-45.

Mita M, Yanagihara H, Hishinuma S, Saito M and Walsh MP (2002) Membrane depolarization-induced contraction of rat caudal arterial smooth muscle involves Rho-associated kinase. *Biochem J* 364(Pt 2): 431-440.

Moffat LD, Brown SB, Grassie ME, Ulke-Lemee A, Williamson LM, Walsh MP and MacDonald JA (2011) Chemical genetics of zipper-interacting protein kinase reveal myosin light chain as a bona fide substrate in permeabilized arterial smooth muscle. *J Biol Chem* 286(42): 36978-36991.

Murata-Hori M, Suizu F, Iwasaki T, Kikuchi A and Hosoya H (1999) ZIP kinase identified as a novel myosin regulatory light chain kinase in HeLa cells. *FEBS Lett* 451(1): 81-84.

Ngai PK, Carruthers CA and Walsh MP (1984) Isolation of the native form of chicken gizzard myosin light-chain kinase. *Biochem J* 218(3): 863-870.

Niiro N and Ikebe M (2001) Zipper-interacting protein kinase induces Ca(2+)-free smooth muscle contraction via myosin light chain phosphorylation. *J Biol Chem* 276(31): 29567-29574.

Okamoto M, Takayama K, Shimizu T, Ishida K, Takahashi O and Furuya T (2009) Identification of death-associated protein kinases inhibitors using structure-based virtual screening. *J Med Chem* 52(22): 7323-7327.

Okamoto M, Takayama K, Shimizu T, Muroya A and Furuya T (2010) Structure-activity relationship of novel DAPK inhibitors identified by structure-based virtual screening. *Bioorg Med Chem* 18(7): 2728-2734.

Puetz S, Lubomirov LT and Pfitzer G (2009) Regulation of smooth muscle contraction by small GTPases. *Physiology (Bethesda)* 24: 342-356.

Sakamoto K, Hori M, Izumi M, Oka T, Kohama K, Ozaki H and Karaki H (2003) Inhibition of high K+-induced contraction by the ROCKs inhibitor Y-27632 in vascular smooth muscle: possible involvement of ROCKs in a signal transduction pathway. *J Pharmacol Sci* 92(1): 56-69.

Sakurada S, Takuwa N, Sugimoto N, Wang Y, Seto M, Sasaki Y and Takuwa Y (2003) Ca2+-dependent activation of Rho and Rho kinase in membrane depolarization-induced and receptor stimulation-induced vascular smooth muscle contraction. *Circ Res* 93(6): 548-556.

Shani G, Marash L, Gozuacik D, Bialik S, Teitelbaum L, Shohat G and Kimchi A (2004) Death-associated protein kinase phosphorylates ZIP kinase, forming a unique

kinase hierarchy to activate its cell death functions. *Mol Cell Biol* 24(19): 8611-8626.

Shiloh R, Bialik S and Kimchi A (2014) The DAPK family: a structure-function analysis. *Apoptosis* 19(2): 286-297.

Sutera SP and Skalak R (1993) The History of Poiseuille's Law. *Ann Rev Fluid Mech* 25: 1-20.

Sutherland C and Walsh MP (2012) Myosin regulatory light chain diphosphorylation slows relaxation of arterial smooth muscle. *J Biol Chem* 287(29): 24064-24076.

Takamoto N, Komatsu S, Komaba S, Niiro N and Ikebe M (2006) Novel ZIP kinase isoform lacks leucine zipper. *Arch Biochem Biophys* 456(2): 194-203.

Takeya K, Loutzenhiser K, Shiraishi M, Loutzenhiser R and Walsh MP (2008) A highly sensitive technique to measure myosin regulatory light chain phosphorylation: the first quantification in renal arterioles. *Am J Physiol Renal Physiol* 294(6): F1487-1492.

Takeya K, Wang X, Sutherland C, Kathol I, Loutzenhiser K, Loutzenhiser RD and Walsh MP (2014) Involvement of myosin regulatory light chain diphosphorylation in sustained vasoconstriction under pathophysiological conditions. *J Smooth Muscle Res* 50: 18-28.

Uehata M, Ishizaki T, Satoh H, Ono T, Kawahara T, Morishita T, Tamakawa H, Yamagami K, Inui J, Maekawa M and Narumiya S (1997) Calcium sensitization of smooth muscle mediated by a Rho-associated protein kinase in hypertension. *Nature* 389(6654): 990-994.

Urban NH, Berg KM and Ratz PH (2003) K+ depolarization induces RhoA kinase translocation to caveolae and Ca2+ sensitization of arterial muscle. *Am J Physiol Cell Physiol* 285(6): C1377-1385.

Usui T, Okada M and Yamawaki H (2014) Zipper interacting protein kinase (ZIPK): function and signaling. *Apoptosis* 19(2): 387-391.

Velentza AV, Wainwright MS, Zasadzki M, Mirzoeva S, Schumacher AM, Haiech J, Focia PJ, Egli M and Watterson DM (2003) An aminopyridazine-based inhibitor of a pro-apoptotic protein kinase attenuates hypoxia-ischemia induced acute brain injury. *Bioorg Med Chem Lett* 13(20): 3465-3470.

Vetterkind S, Lee E, Sundberg E, Poythress RH, Tao TC, Preuss U and Morgan KG (2010) Par-4: a new activator of myosin phosphatase. *Mol Biol Cell* 21(7): 1214-1224.

Vetterkind S and Morgan KG (2009) The pro-apoptotic protein Par-4 facilitates vascular contractility by cytoskeletal targeting of ZIPK. *J Cell Mol Med* 13(5): 887-895.

Weber LP, Van Lierop JE and Walsh MP (1999) Ca2+-independent phosphorylation of myosin in rat caudal artery and chicken gizzard myofilaments. *J Physiol* 516 (Pt 3): 805-824.

Wettschureck N and Offermanns S (2005) Mammalian G proteins and their cell type specific functions. *Physiol Rev* 85(4): 1159-1204.

Wilson DP, Susnjar M, Kiss E, Sutherland C and Walsh MP (2005a) Thromboxane A2-induced contraction of rat caudal arterial smooth muscle involves activation of Ca2+ entry and Ca2+ sensitization: Rho-associated kinase-mediated

phosphorylation of MYPT1 at Thr-855, but not Thr-697. *Biochem J* 389(Pt 3): 763-774.

Wilson DP, Sutherland C, Borman MA, Deng JT, Macdonald JA and Walsh MP (2005b) Integrin-linked kinase is responsible for Ca2+-independent myosin diphosphorylation and contraction of vascular smooth muscle. *Biochem J* 392(Pt 3): 641-648.

Wynne BM, Chiao CW and Webb RC (2009) Vascular Smooth Muscle Cell Signaling Mechanisms for Contraction to Angiotensin II and Endothelin-1. *J Am Soc Hypertens* 3(2): 84-95.

Xu J, Yang G, Li T, Ming J and Liu L (2010) Involvement of Cpi-17 and zipper-interacting protein kinase in the regulation of protein kinase C-alpha, protein kinase C-epsilon on vascular calcium sensitivity after hemorrhagic shock. *Shock* 33(1): 49-55.

Footnotes

This work was supported by the Heart and Stroke Foundation of Canada, the Canadian Institutes of Health Research [Grant MOP-111262], the Swedish Scientific Research Council, the Alberta Innovates – Health Solutions Independent Investigator Award Program, the Canada Research Chairs Program, and the Mandel Foundation.

Molecular Pharmacology Fast Forward. Published on October 13, 2015 as DOI: 10.1124/mol.115.100529
This article has not been copyedited and formatted. The final version may differ from this version.

Legends for Figures

FIGURE 1. The effects of HS38 on the activities of Rho-associated kinase and myosin light chain kinase, and the rate of force development and maximal tension elicited by the phosphatase inhibitor calyculin A. ***A*** and ***B***, effects of increasing concentrations of HS38 on the activities of ROCK2 and MLCK, respectively. ***C*** and ***D***, representative contractile responses of de-endothelialized rat caudal arterial smooth muscle strips to calyculin A (CLa, 0.5 μM) in the presence of vehicle (1% DMSO) or HS38 (50 μM), respectively. ***E***, the time required to reach half-maximal contraction ($t_{1/2}$) after application of CLa in the presence of increasing concentrations of HS38 was calculated and normalized to the value in the absence of HS38. #significantly different from the value in the absence of HS38 (ANOVA, Dunnett's *post hoc* test, $p < 0.05$). ***F***, the maximal contractile force developed during CLa exposure (0.5 μM for 60 min) at different concentrations of HS38 was expressed as a percentage of the initial reference contraction to 87 mM KCl. Values in (***E***) and (***F***) indicate the mean ± S.E.M. (n = 4-7).

FIGURE 2. Reversibility of the inhibitory effect of HS38 on calyculin A-induced contraction. De-endothelialized rat caudal arterial smooth muscle strips in H-T buffer were pre-incubated for 30 min (***A***) or 3 h (***B***) with vehicle (DMSO) or HS38 (100 μM). HS38 was retained or washed out for 30 min prior to addition of CLa (0.5 μM) for 3 h to elicit a sustained contractile response. The time required to reach half-maximal force ($t_{1/2}$) was calculated and normalized to the vehicle control, which had never seen HS38. Values indicate the mean ± S.E.M. (n = 3) with the control value set at 100%. *significantly different from the force evoked in the absence of HS38 (vehicle control). #significantly different from the force evoked in the presence of HS38. *nsd* no significant difference

Molecular Pharmacology Fast Forward. Published on October 13, 2015 as DOI: 10.1124/mol.115.100529
This article has not been copyedited and formatted. The final version may differ from this version.

from vehicle control. Statistical significance assessed by ANOVA with Dunnett's *post hoc* test, $p<0.05$).

FIGURE 3. The effect of HS38 on calyculin A-induced LC_{20} phosphorylation. LC_{20} phosphorylation was analyzed by Phos-Tag SDS-PAGE with detection of unphosphorylated (LC_{20}-0P), mono (LC_{20}-1P)-, di (LC_{20}-2P)- and tri (LC_{20}-3P)-phosphorylated forms of LC_{20} by western blotting with anti-LC_{20}. ***A***, the effect of increasing concentrations of HS38 on LC_{20} phosphorylation induced by CLa treatment (0.5 μM for 60 min). A representative western blot is shown above cumulative quantitative data. Phosphorylation stoichiometry (mol P_i/mol LC_{20}) was calculated as described under *Experimental Procedures*. ***B*** and ***C***, representative western blots and cumulative quantitative data showing the time courses of LC_{20} phosphorylation in response to CLa (0.5 μM) in the presence of vehicle (DMSO) (***B***) or HS38 (100 μM) (***C***). The various LC_{20} bands were quantified by scanning densitometry and expressed as a percentage of the total LC_{20} signal. ***D***, LC_{20} phosphorylation stoichiometry is expressed as mol P_i/mol LC_{20}. $^{\#}$significantly different from the corresponding value in the absence of HS38 (ANOVA with Dunnett's *post hoc* test, $p<0.05$). Values in (***A***) and (***B***-***D***) indicate the mean ± S.E.M. (n = 4-7 in (***A***) and n = 4 in (***B***-***D***)).

FIGURE 4. The effect of HS38 on calyculin A-induced phosphorylation of MYPT1 at Thr697 and Thr855. The time-courses of MYPT1 phosphorylation at Thr697 (***A*** - ***C***) and Thr855 (***D*** - ***E***) were analyzed by SDS-PAGE and western blotting with phosphospecific antibodies following stimulation of caudal arterial smooth muscle strips with CLa (0.5 μM) in the presence of vehicle (DMSO) (***A*** and ***D***) or HS38 (100 μM) (***B*** and ***E***). Cumulative quantitative data showing the time-course of MYPT1

Molecular Pharmacology Fast Forward. Published on October 13, 2015 as DOI: 10.1124/mol.115.100529
This article has not been copyedited and formatted. The final version may differ from this version.

phosphorylation (fold-increase relative to levels at time zero) for Thr697 (***C***) and Thr855 (***F***) in the absence and presence of HS38 (100 μM) are provided. α-actin was used as the loading control. Data are representative of 4 independent experiments. *- Statistical significance assessed with the Student's *t* test (two-tailed), $p<0.05$.

FIGURE 5. The effect of HS38 on calyculin A-induced phosphorylation of CPI-17. ***A***, the time-course of CPI-17 phosphorylation was analyzed by Phos-Tag SDS-PAGE and western blotting with anti-CPI-17 following stimulation of caudal arterial smooth muscle strips with CLa (0.5 μM), and in the presence of vehicle or HS38 (100 μM). ***B,*** cumulative quantitative data showing the time-course of CPI-17 phosphorylation (mol P_i/mol CPI-17) in the absence and presence of HS38 (100 μM). Values indicate the mean ± S.E.M. (n = 5).

FIGURE 6. The effect of HS38 on calyculin A-induced phosphorylation of Par-4. The time-course of Par-4 phosphorylation was analyzed by Phos-Tag SDS-PAGE and western blotting with anti-Par-4 following stimulation of caudal arterial smooth muscle strips with CLa (0.5 μM) in the presence of vehicle (DMSO) (***A***) or HS38 (100 μM) (***B***). ***C***, the Par-4 bands were quantified by scanning densitometry, and the data are expressed as the phosphorylation stoichiometry (mol P_i/mol Par-4) calculated as described for LC_{20} phosphorylation under *Experimental Procedures*. Values indicate the mean ± S.E.M. (n = 4).

FIGURE 7. The effect of PIM kinase inhibitor HS43 on calyculin A-induced contraction and phosphorylation of LC_{20}, Par-4 and MYPT1. ***A***, de-endothelialized rat caudal arterial smooth muscle strips were treated with CLa (0.5 μM) in the presence

Molecular Pharmacology Fast Forward. Published on October 13, 2015 as DOI: 10.1124/mol.115.100529
This article has not been copyedited and formatted. The final version may differ from this version.

of vehicle (DMSO), HS38 (100 μM) or HS43 (100 μM). The force was recorded continuously for the calculation of $t_{1/2}$ (time required to reach half-maximal force) (***B***) and maximal force (***C***). LC_{20} (***D***) and Par-4 phosphorylations (***E*** and ***F***) were quantified by Phos-Tag SDS-PAGE and western blotting of tissues harvested at maximal force. MYPT1 phosphorylation at Thr697 and Thr855 was analyzed by western blotting with phosphospecific antibodies (***G*** and ***H***). Values in (***B***-***D***), (***F***) and (***H***) indicate the mean ± S.E.M. (n = 3). *significantly different from the $t_{1/2}$ value found with vehicle. # significantly different from the $t_{1/2}$ value evoked with HS38. Statistical significance was assessed by ANOVA with Dunnett's *post hoc* test, $p<0.05$.

FIGURE 8. The effect of HS38 on phasic and tonic force development in rat caudal arterial smooth muscle strips treated with various contractile agonists. ***A***, contractile responses of de-endothelialized rat caudal arterial smooth muscle strips were recorded in the absence and presence of HS38 (100 μM) with stimulation by: (*i*) phenylephrine (PE, 1 μM); (*ii*) endothelin-1 (ET-1, 0.1 μM); (*iii*) high-[K^+] extracellular solution (87 mM KCl); (*iv*) thromboxane A_2 mimetic (U46619, 1 μM); (*v*) angiotensin II (AngII, 0.1 μM); and (*vi*) CLa (0.5 μM). The force generated relative to the peak of the initial contraction induced by KCl was calculated from the individual contraction profiles. Tissues were quick-frozen upon reaching peak force in the initial phasic contraction (▼) or upon reaching the sustained tonic contraction maintained at the end of the trace (▽). Values (mean ± S.E.M., n = 3) are provided for the contractile force measured for the phasic (***B***) and tonic (***C***) components. *significantly different from the force evoked in the absence of HS38 (Student's *t* test, two-tailed, $p<0.05$).

Molecular Pharmacology Fast Forward. Published on October 13, 2015 as DOI: 10.1124/mol.115.100529
This article has not been copyedited and formatted. The final version may differ from this version.

FIGURE 9. The effect of HS38 on phosphorylation of LC_{20}, MYPT1 and CPI-17 evoked by various agonists. De-endothelialized rat caudal arterial smooth muscle strips were treated with the indicated agonists in the absence or presence of HS38 (100 μM): phenylephrine (PE, 1 μM); thromboxane A_2 mimetic (U46619, 1 μM); high-[K^+] extracellular solution (87 mM KCl); angiotensin II (AngII, 0.1 μM); and endothelin-1 (ET-1, 0.1 μM). Tissues were quick frozen for western blot analysis at the peak of contraction (PE and KCl: 1 min; U46619, AngII and ET-1: 5 min). ***A***, LC_{20} phosphorylation was analyzed by Phos-Tag SDS-PAGE and western blotting with anti-LC_{20}. ***B***, immunoreactive bands from (***A***) were quantified by scanning densitometry and phosphorylation stoichiometry (mol P_i/mol LC_{20}) was calculated as described under *Experimental Procedures*. ***C***, The phosphorylation of MYPT1 at Thr697 and Thr855 was analyzed by western blotting with phosphospecific antibodies using α-actin as a loading control. Cumulative quantitative data are presented in (***D***) as the % change in Thr697 or Thr855 phosphorylation with treatment of HS38 relative to agonist in the presence of vehicle control. ***E***, CPI-17 phosphorylation was analyzed by Phos-Tag SDS-PAGE and western blotting with anti-CPI-17. ***F***, CPI-17 bands were quantified by scanning densitometry and phosphorylation stoichiometry (mol P_i/mol CPI-17) was calculated as described for LC_{20} under *Experimental Procedures*. VSM strips treated with CLa (0.5 mM for 60 min) were used as positive controls in (***A***), (***C***) and (***E***). Values indicate the mean ± S.E.M. (n = 3). $^{\#}$significantly different from phosphorylation levels under resting conditions (tissue incubated in H-T buffer); *significantly different from agonist stimulation in the absence of HS38 using the Student's t test (two-tailed), $p<0.05$.

FIGURE 10. Proposed signaling mechanisms for the regulation of vascular smooth

Molecular Pharmacology Fast Forward. Published on October 13, 2015 as DOI: 10.1124/mol.115.100529
This article has not been copyedited and formatted. The final version may differ from this version.

muscle contraction by ZIPK. The coupling of agonist-activated G protein-coupled receptors (GPCRs) to phospholipase Cβ (PLCβ) via the heterotrimeric G protein $G_{q/11}$ results in the hydrolysis of phosphatidylinositol 4,5-bisphosphate (PIP_2) to inositol 1,4,5-trisphosphate (IP_3), which releases Ca^{2+} from the sarcoplasmic reticulum (SR) via IP_3 receptors (Ca^{2+} channels) in the SR membrane. This results in activation of Ca^{2+}/calmodulin (CaM)-dependent myosin light chain kinase (MLCK), which phosphorylates the 20 kDa regulatory light chains of myosin II at Ser19. Agonist stimulation of GPCRs also results in the activation of Rho-associated coiled coil-containing protein kinase (ROCK) via $G_{12/13}$, a Rho-guanine nucleotide exchange factor (RhoGEF) and the small GTPase RhoA. Activated ROCK leads to inhibition of myosin light chain phosphatase (MLCP) activity, increased LC_{20} phosphorylation and smooth muscle contraction. VSM contraction can be evoked independently of Ca^{2+} by direct phosphorylation of MYPT1 (the myosin-targeting subunit of MLCP) at Thr697 and Thr855, or indirectly via phosphorylation of CPI-17 (PKC-potentiated inhibitory protein for protein phosphatase type 1 of 17-kDa) at Thr38. Two discrete pools of ZIPK play distinct roles in Ca^{2+} sensitization of VSM contraction: (i) a pool of constitutively-active ZIPK (indicated in green), whose activity is unmasked by inhibition of MLCP activity by, for example, calyculin A, phosphorylates LC_{20} at Thr18 and Ser19, and (ii) a pool of ZIPK (indicated in blue) is activated by phosphorylation by ROCK, leading to phosphorylation of MYPT1 and CPI-17 and decreased MLCP activity. Other kinases, including integrin-linked kinase (ILK), can also phosphorylate LC_{20} at Thr18 and Ser19, as well as CPI-17 at Thr38 and MYPT1 at Thr697 and Thr855.

Molecular Pharmacology Fast Forward. Published on October 13, 2015 as DOI: 10.1124/mol.115.100529
This article has not been copyedited and formatted. The final version may differ from this version.

Table 1. Effect of HS38 on contractile responses of rat caudal artery following stimulation with calyculin A.

Parameter	Control (*n* = 94)	HS38 (*n* = 28)
Latency (s)	361.0 ± 15.1 (146.1)	*654.7 ± 60.6 (320.4)
$t_{1/2}$ from stimulation (s)	1082.9 ± 37.9 (367.0)	*1792.0 ± 110.8 (586.1)
$t_{1/2}$ from contraction (s)	702.0 ± 25.6 (248.5)	*1170.1 ± 64.0 (338.9)
% KCl contraction	159.3 ± 5.1 (49.0)	**161.7 ± 8.4 (44.7)

"Control" denotes calyculin A (0.5 μM) alone, "HS38" denotes calyculin A + HS38 (50 μM). Values indicate mean ± SEM (SD). Significantly different from control by Student's unpaired *t* test: *$p < 0.0001$, **$p = 0.81$.

FIGURE 1

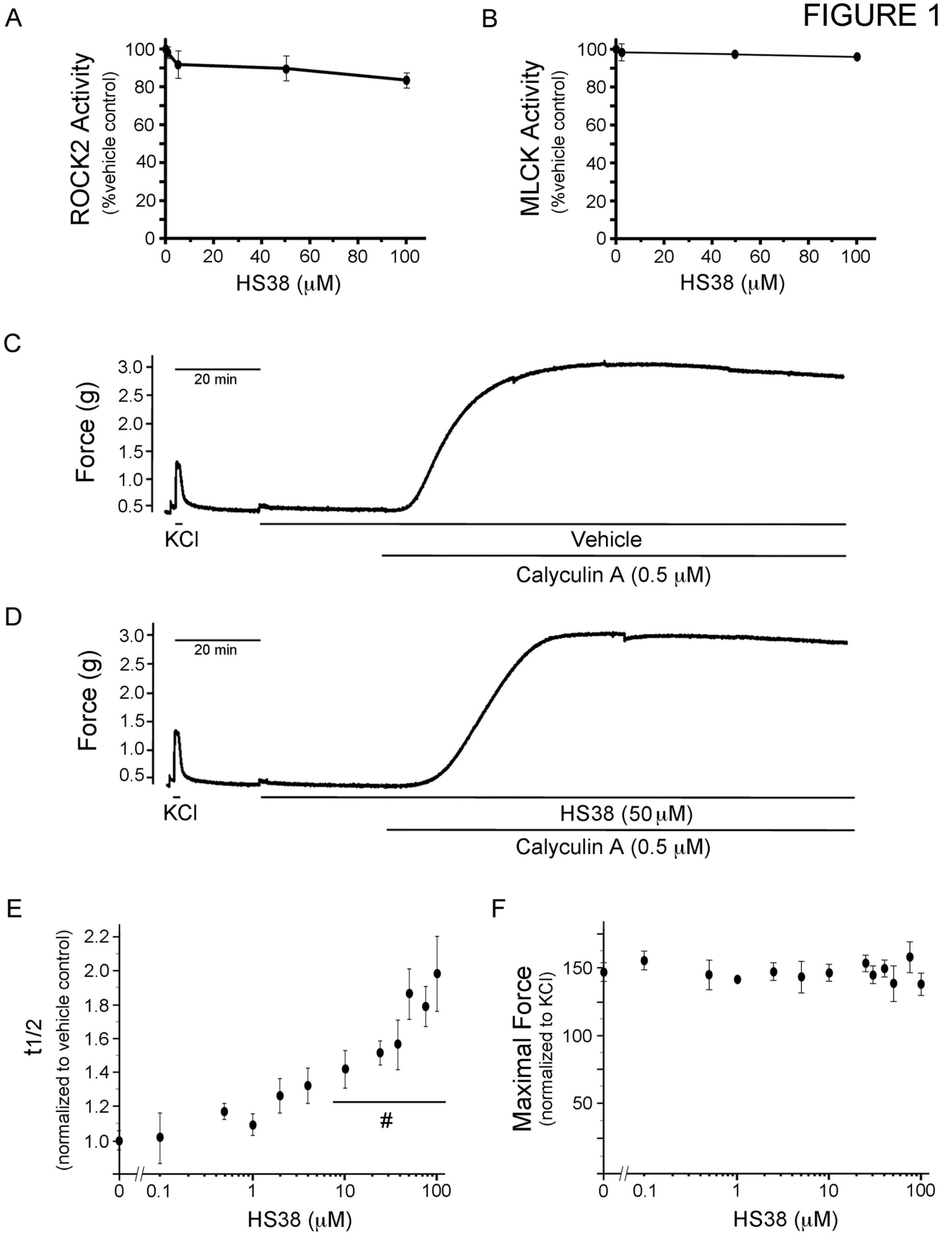
A
ROCK2 Activity
(%vehicle control)
HS38 (μM)
B
MLCK Activity
(%vehicle control)
HS38 (μM)
C
Force (g)
20 min
KCl
Vehicle
Calyculin A (0.5 μM)
D
Force (g)
20 min
KCl
HS38 (50 μM)
Calyculin A (0.5 μM)
E
t1/2
(normalized to vehicle control)
#
HS38 (μM)
F
Maximal Force
(normalized to KCl)
HS38 (μM)

FIGURE 2

A

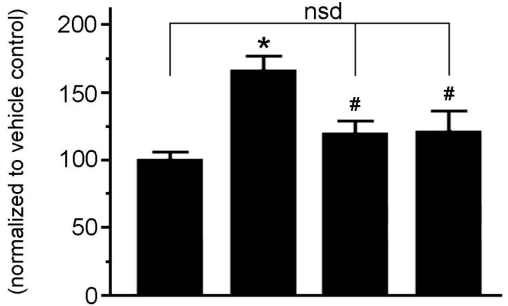

Treatment (30 min):	Vehicle	HS38	Vehicle	HS38
Washout (30 min):	-	-	+	+
CLa (3 h):	+	+	+	+

B

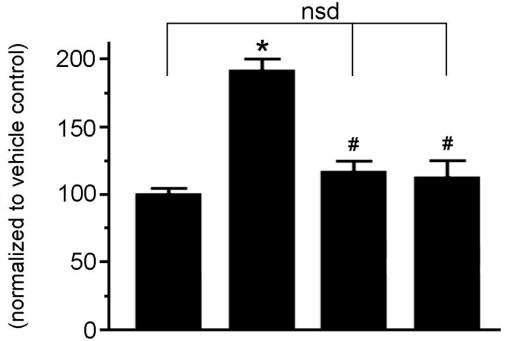

Treatment (3 h):	Vehicle	HS38	Vehicle	HS38
Washout (30 min):	-	-	+	+
CLa (3 h):	+	+	+	+

FIGURE 3

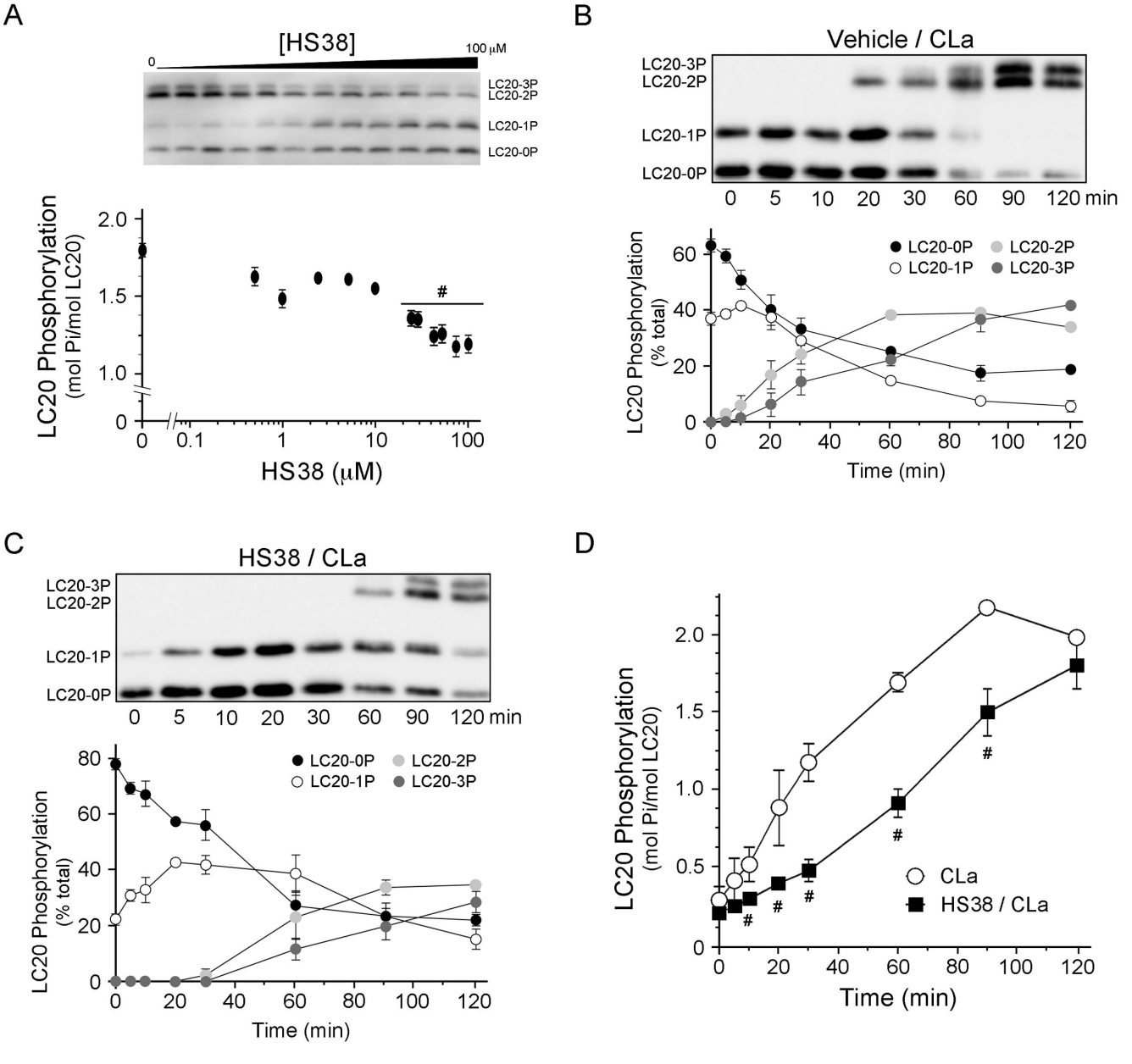
A
[HS38]
0
100 μM
LC20-3P
LC20-2P
LC20-1P
LC20-0P
LC20 Phosphorylation
(mol Pi/mol LC20)
2.0
1.5
1.0
0
0
0.1
1
10
100
HS38 (μM)
#
B
Vehicle / CLa
LC20-3P
LC20-2P
LC20-1P
LC20-0P
0 5 10 20 30 60 90 120 min
LC20 Phosphorylation
(% total)
60
40
20
0
0 20 40 60 80 100 120
Time (min)
LC20-0P
LC20-1P
LC20-2P
LC20-3P
C
HS38 / CLa
LC20-3P
LC20-2P
LC20-1P
LC20-0P
0 5 10 20 30 60 90 120 min
LC20 Phosphorylation
(% total)
80
60
40
20
0
0 20 40 60 80 100 120
Time (min)
LC20-0P
LC20-1P
LC20-2P
LC20-3P
D
LC20 Phosphorylation
(mol Pi/mol LC20)
2.0
1.5
1.0
0.5
0
0 20 40 60 80 100 120
Time (min)
CLa
HS38 / CLa
#
#
#
#
#

FIGURE 4

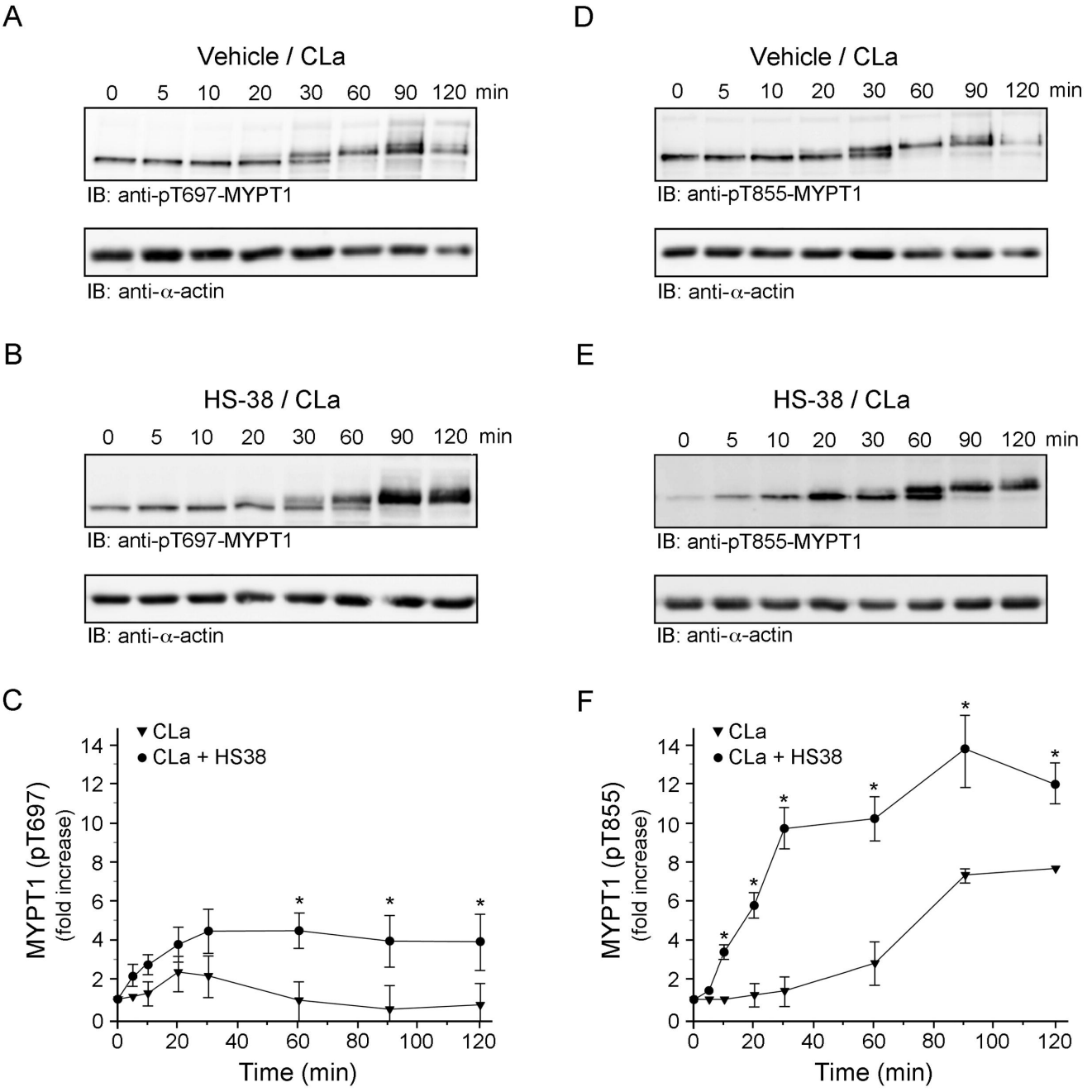
A
Vehicle / CLa
0 5 10 20 30 60 90 120 min
IB: anti-pT697-MYPT1
IB: anti-α-actin
D
Vehicle / CLa
0 5 10 20 30 60 90 120 min
IB: anti-pT855-MYPT1
IB: anti-α-actin
B
HS-38 / CLa
0 5 10 20 30 60 90 120 min
IB: anti-pT697-MYPT1
IB: anti-α-actin
E
HS-38 / CLa
0 5 10 20 30 60 90 120 min
IB: anti-pT855-MYPT1
IB: anti-α-actin
C
CLa
CLa + HS38
MYPT1 (pT697)
(fold increase)
Time (min)
F
CLa
CLa + HS38
MYPT1 (pT855)
(fold increase)
Time (min)

FIGURE 5

A

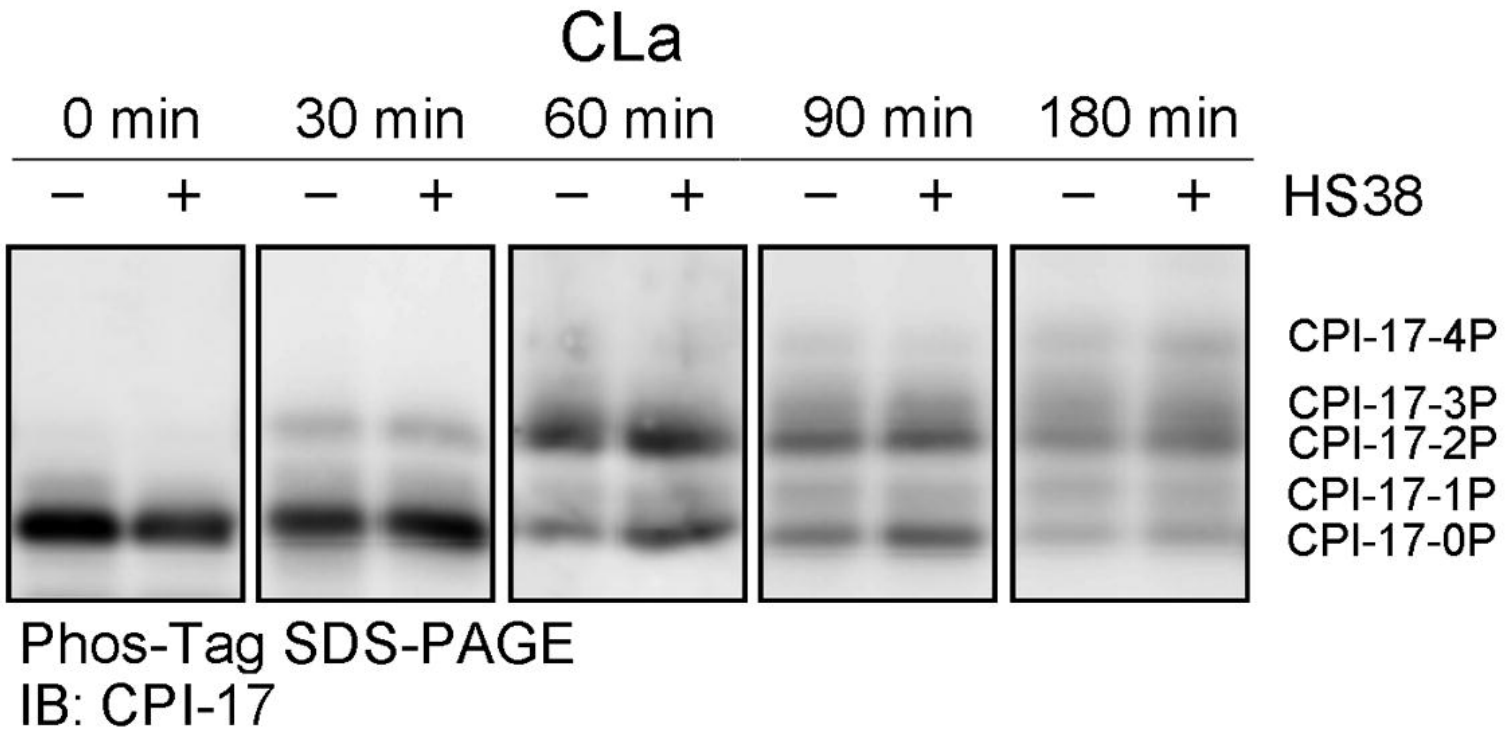
CLa
0 min
30 min
60 min
90 min
180 min
– + – + – + – + – +
HS38
CPI-17-4P
CPI-17-3P
CPI-17-2P
CPI-17-1P
CPI-17-0P
Phos-Tag SDS-PAGE
IB: CPI-17

B

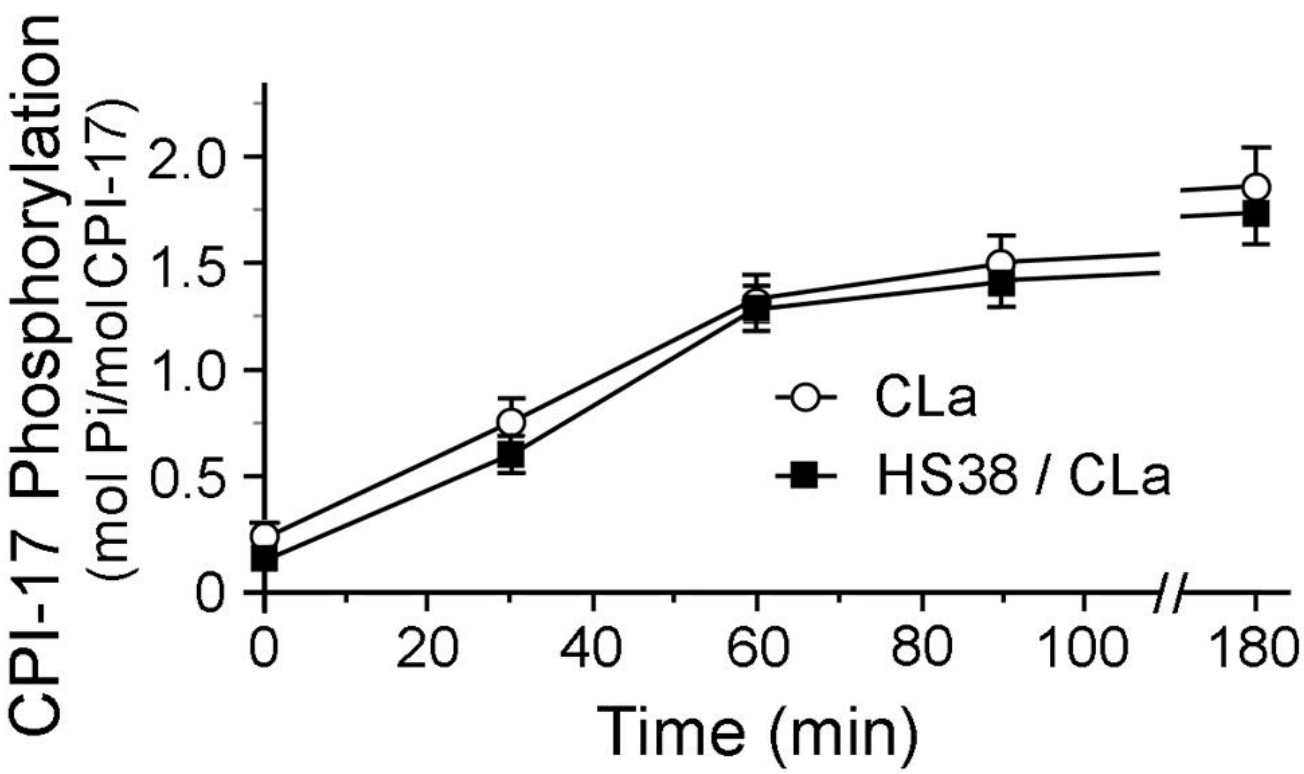
CPI-17 Phosphorylation
(mol Pi/mol CPI-17)
2.0
1.5
1.0
0.5
0
0
20
40
60
80
100
180
Time (min)
CLa
HS38 / CLa

FIGURE 6

A

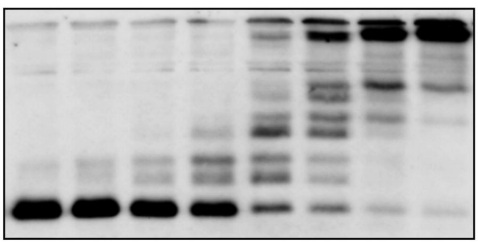

Phos-Tag SDS-PAGE
IB: anti-Par-4

B

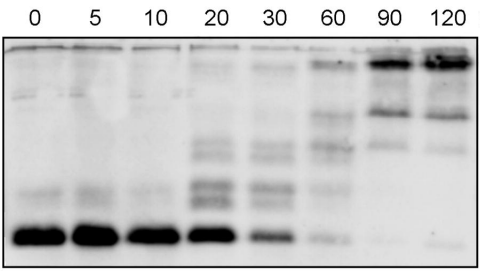

Phos-Tag SDS-PAGE
IB: anti-Par-4

C

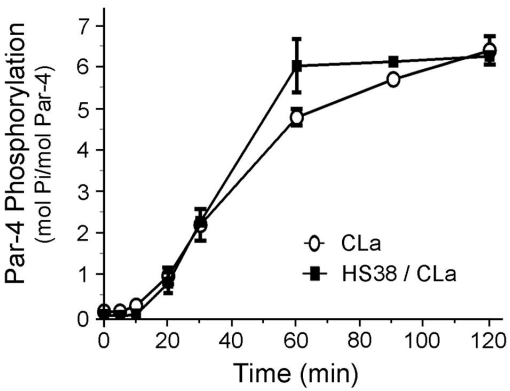

FIGURE 7

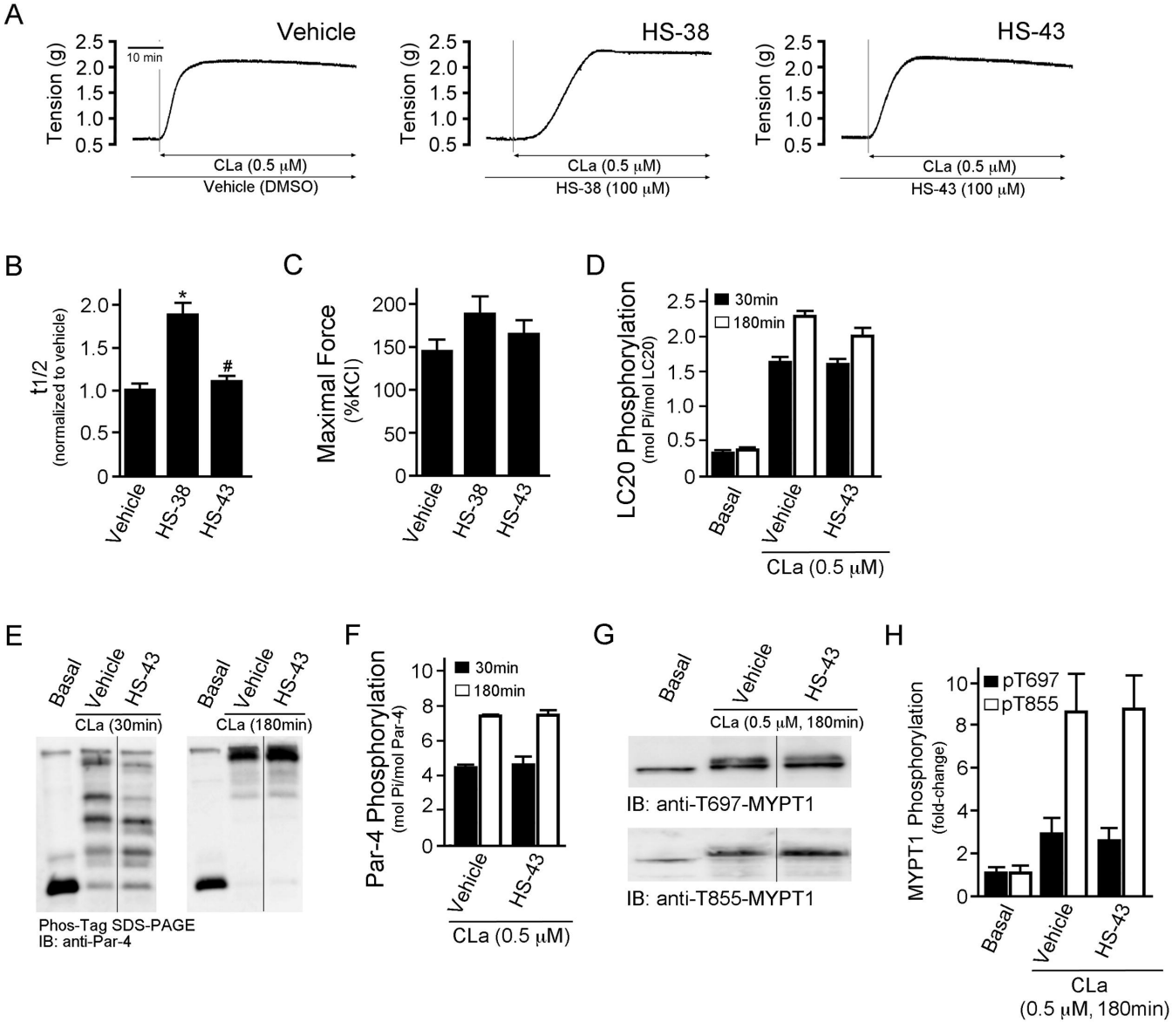
A
Vehicle
HS-38
HS-43
Tension (g)
10 min
CLa (0.5 μM)
Vehicle (DMSO)
HS-38 (100 μM)
HS-43 (100 μM)
B
t1/2
(normalized to vehicle)
C
Maximal Force
(%KCl)
D
LC20 Phosphorylation
(mol Pi/mol LC20)
30min
180min
Basal
CLa (0.5 μM)
E
CLa (30min)
CLa (180min)
Phos-Tag SDS-PAGE
IB: anti-Par-4
F
Par-4 Phosphorylation
(mol Pi/mol Par-4)
G
CLa (0.5 μM, 180min)
IB: anti-T697-MYPT1
IB: anti-T855-MYPT1
H
MYPT1 Phosphorylation
(fold-change)
pT697
pT855
CLa
(0.5 μM, 180min)

FIGURE 8

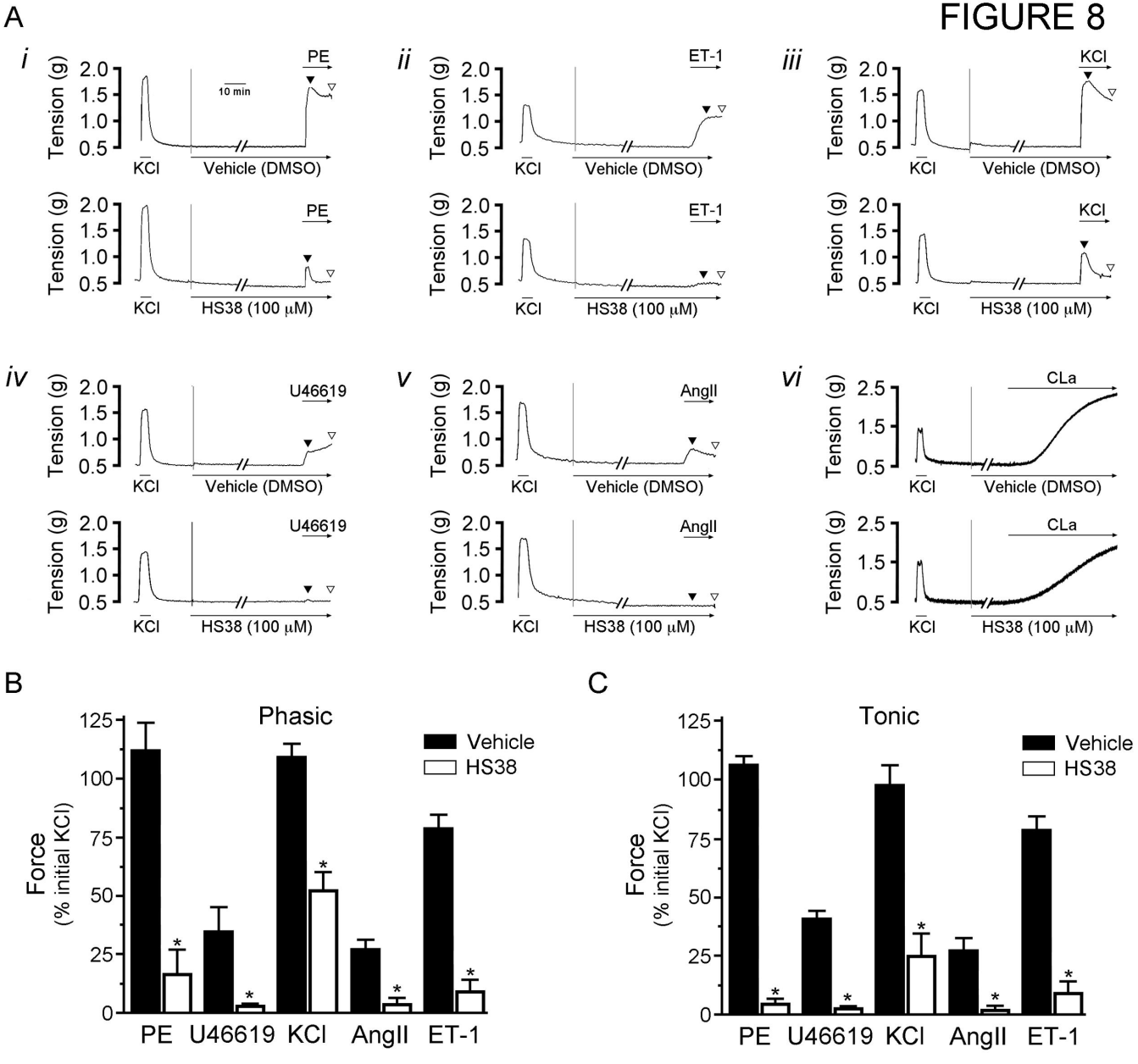
A
i
ii
iii
iv
v
vi
Tension (g)
2.0
1.5
1.0
0.5
2.5
10 min
PE
ET-1
KCl
U46619
AngII
CLa
KCl
Vehicle (DMSO)
HS38 (100 μM)
B
Phasic
C
Tonic
Vehicle
HS38
Force
(% initial KCl)
125
100
75
50
25
0
*
PE
U46619
KCl
AngII
ET-1

FIGURE 9

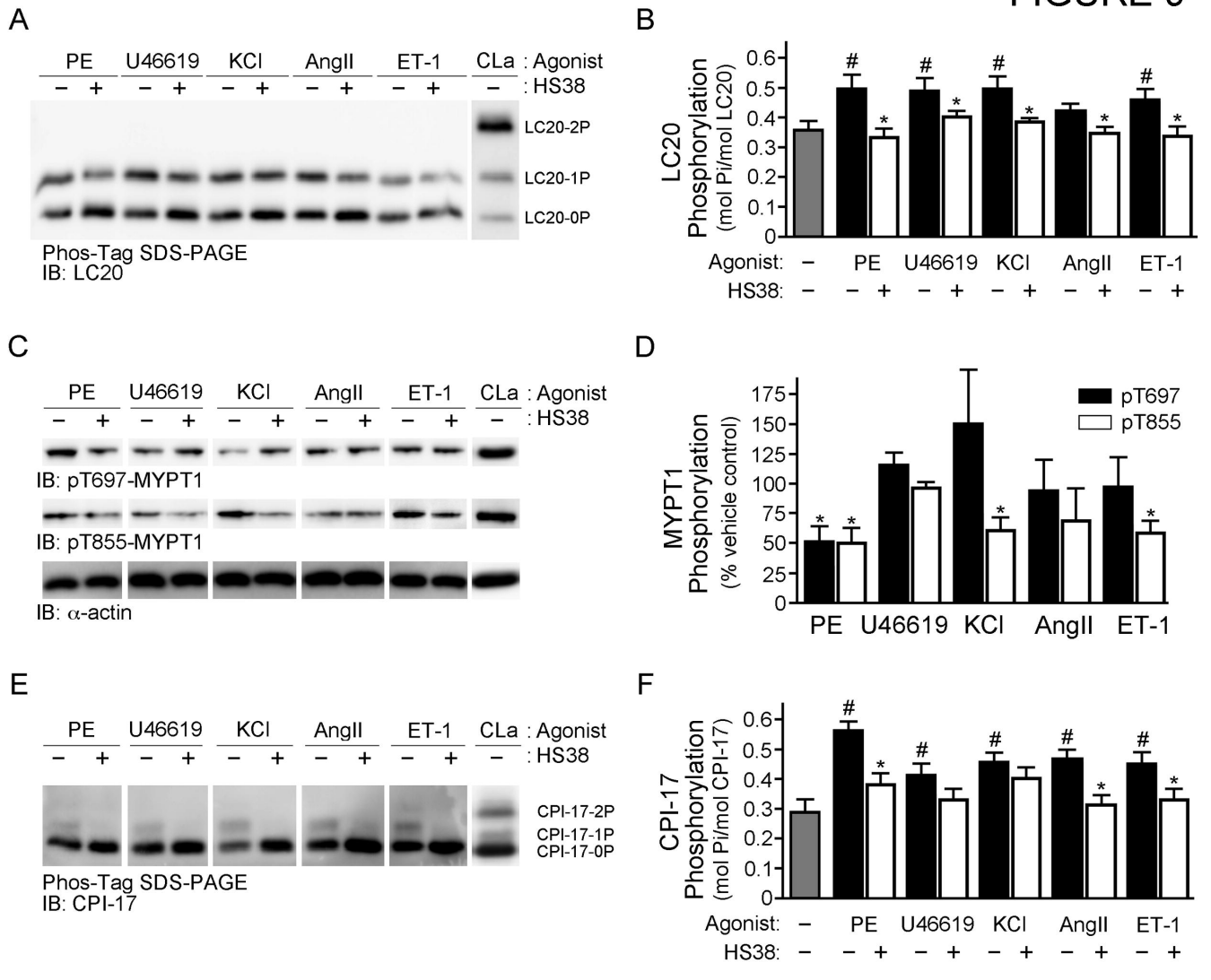
A
PE
U46619
KCl
AngII
ET-1
CLa
: Agonist
: HS38
LC20-2P
LC20-1P
LC20-0P
Phos-Tag SDS-PAGE
IB: LC20
B
LC20 Phosphorylation (mol Pi/mol LC20)
Agonist:
HS38:
C
IB: pT697-MYPT1
IB: pT855-MYPT1
IB: α-actin
D
MYPT1 Phosphorylation (% vehicle control)
pT697
pT855
E
CPI-17-2P
CPI-17-1P
CPI-17-0P
Phos-Tag SDS-PAGE
IB: CPI-17
F
CPI-17 Phosphorylation (mol Pi/mol CPI-17)

FIGURE 10

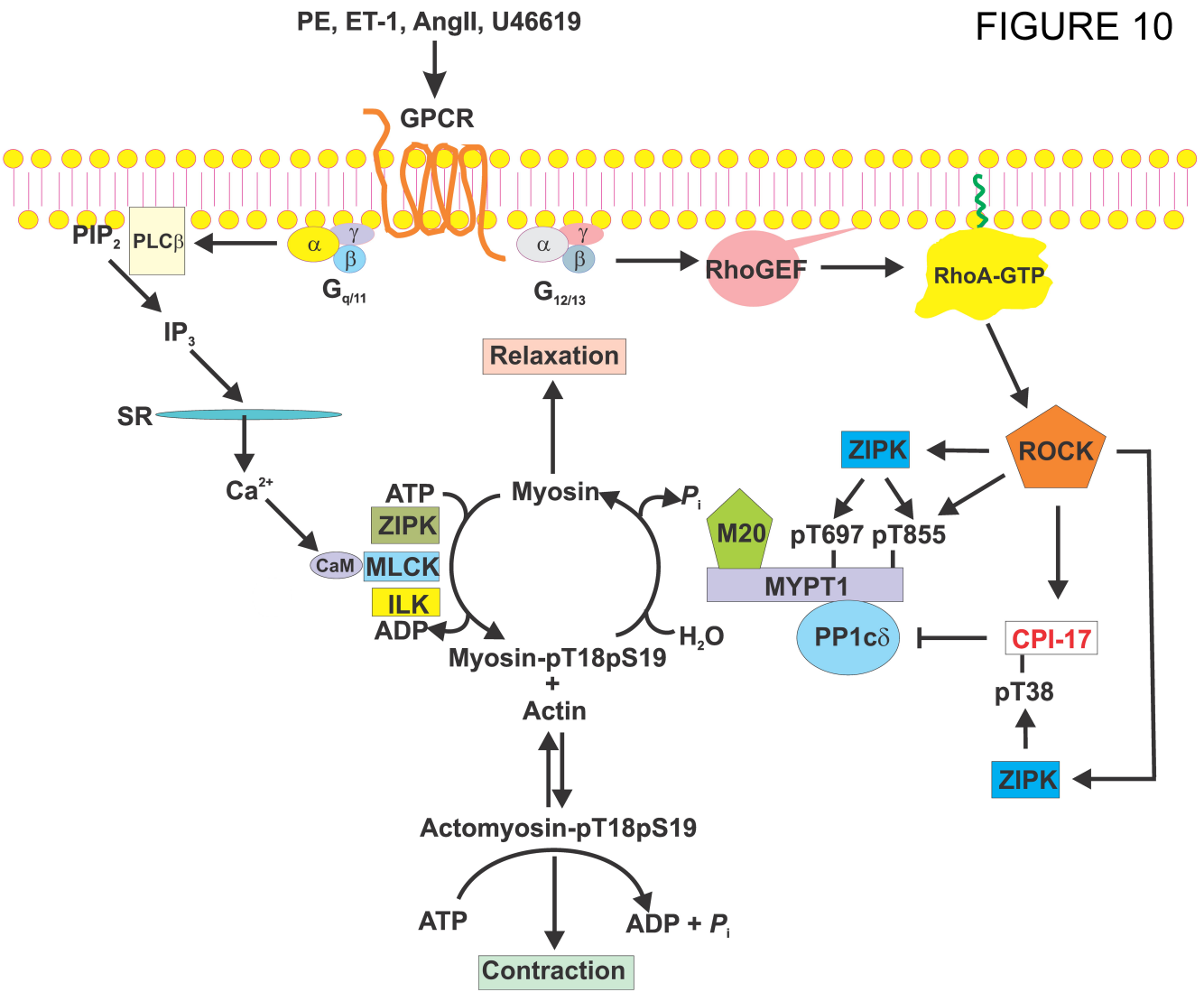
PE, ET-1, AngII, U46619
GPCR
PIP2
PLCβ
α
γ
β
Gq/11
G12/13
RhoGEF
RhoA-GTP
IP3
SR
Ca2+
CaM
MLCK
ZIPK
ILK
ATP
ADP
Myosin
Pi
H2O
Relaxation
Myosin-pT18pS19
+
Actin
Actomyosin-pT18pS19
ATP
ADP + Pi
Contraction
ROCK
ZIPK
M20
pT697 pT855
MYPT1
PP1cδ
CPI-17
pT38
ZIPK